HHS Public Access

Author manuscript

Sci Signal. Author manuscript; available in PMC 2018 March 19.

Published in final edited form as:

Sci Signal. ; 10(497): . doi:10.1126/scisignal.aan2883.

TALK-1 channels control β cell endoplasmic reticulum Ca^{2+} homeostasis

Nicholas C. Vierra[1], **Prasanna K. Dadi**[1], **Sarah C. Milian**[1], **Matthew T. Dickerson**[1], **Kelli L. Jordan**[1], **Patrick Gilon**[2], and **David A. Jacobson**[1,*]

[1]Department of Molecular Physiology and Biophysics, Vanderbilt University, Nashville, TN 37232, USA

[2]Pôle d'endocrinologie, diabète et nutrition, Institut de recherche expérimentale et clinique, Université catholique de Louvain, 1200 Brussels, Belgium

Abstract

Ca^{2+} handling by the endoplasmic reticulum (ER) serves critical roles controlling pancreatic β-cell function and becomes perturbed during the pathogenesis of diabetes. ER Ca^{2+} homeostasis is determined by ion movements across the ER membrane, including K^+ flux through K^+ channels. Here, we demonstrated that K^+ flux through ER-localized TALK-1 channels facilitated Ca^{2+} release from the ER in mouse and human β-cells. We found that β-cells from mice lacking TALK-1 exhibited reduced basal cytosolic Ca^{2+} and increased ER Ca^{2+} concentrations, suggesting reduced ER Ca^{2+} leak. These changes in Ca^{2+} homeostasis were presumably due to TALK-1-mediated ER K^+ flux, because we recorded K^+ currents mediated by functional TALK-1 channels on the nuclear membrane, which is continuous with the ER. Moreover, overexpression of K^+-impermeable TALK-1 channels in HEK293 cells did not reduce ER Ca^{2+} stores. Reduced ER Ca^{2+} content in β-cells is associated with ER stress and islet dysfunction in diabetes, and islets from TALK-1-deficient mice fed a high-fat diet showed reduced signs of ER stress, suggesting that TALK-1 activity exacerbated ER stress. Our data establish TALK-1 channels as key regulators of β-cell ER Ca^{2+}, and suggest that TALK-1 may be a therapeutic target to reduce ER Ca^{2+} handling defects in β-cells during the pathogenesis of diabetes.

INTRODUCTION

Pancreatic β-cell Ca^{2+} influx triggers insulin secretion, and endoplasmic reticulum (ER) Ca^{2+} (Ca^{2+}_{ER}) handling plays a key role in this process (1). Ca^{2+}_{ER} serves many essential functions in β-cells, such as controlling protein processing and metabolism, and defects in Ca^{2+}_{ER} homeostasis can trigger the unfolded protein response (UPR) (2). The importance of precise β-cell Ca^{2+}_{ER} handling is evident in type-1 and type-2 diabetes mellitus (T2DM), during which Ca^{2+}_{ER} homeostasis is disrupted, leading to β-cell dysfunction and eventual

*Address correspondence to: David A. Jacobson, Department of Molecular Physiology and Biophysics, Vanderbilt University, 7425B MRB IV, 2213 Garland Ave., Nashville, TN, 37232-0615. david.a.jacobson@vanderbilt.edu (D.A.J.); Phone: 615-875-7655.

Author contributions: N.C.V. and D.A.J. designed the project; N.C.V., P.G., and D.A.J developed methodology; N.C.V., P.K.D., S.C.M., M.T.D., K.L.J. and D.A.J. performed experiments and analyzed the data; N.C.V. and D.A.J. wrote and edited the manuscript.

Competing interests: The authors declare that they have no competing interests.

destruction (1–8). Impaired Ca^{2+}_{ER} handling also causes defects in glucose-stimulated insulin secretion (GSIS), contributing to hyperglycemia (3, 9). Therefore, treatments which reduce ER stress in the context of β-cell dysfunction improve glucose tolerance (10–12). However, while it is known that β-cell Ca^{2+}_{ER} concentrations are perturbed in diabetes (2, 4–7), the molecular determinants which set β-cell Ca^{2+}_{ER} are poorly understood.

Maintenance of Ca^{2+}_{ER} homeostasis requires that Ca^{2+} movement across the ER membrane is balanced with a simultaneous K^+ flux in the opposite direction (13–15). Without this K^+ countercurrent, Ca^{2+} release from the ER would rapidly generate a negative charge on the inside of the ER membrane, inhibiting further Ca^{2+}_{ER} release. To date, only a few ER K^+ channels have been identified, including TRIC-A channels, which regulate Ca^{2+}_{ER} stores in myocytes (16, 17); TRIC-B channels, which control Ca^{2+}_{ER} homeostasis in alveolar epithelial cells and osteoblasts (18, 19); and SK Ca^{2+}-activated K^+ channels, which modulate Ca^{2+}_{ER} uptake in neurons and cardiomyocytes (20). Genetic ablation or pharmacological inhibition of these channels impairs Ca^{2+}_{ER} handling. For example, knockout of TRIC-A or TRIC-B channels results in increased Ca^{2+}_{ER} stores, presumably due to the loss of a K^+ countercurrent which regulates the ability of Ca^{2+} to exit the ER (15, 16, 18). Despite the importance of K^+ countercurrents in maintaining Ca^{2+}_{ER} homeostasis, nothing is known about the mediators or functions of β-cell ER K^+ countercurrents.

ER localization has been reported for several K2P channels, including TASK-1 (21), TASK-3 (22), TASK-5 (23), TWIK-2 (24, 25), and THIK-2 (24). Although the subcellular localization of TALK-1 channels has not been reported, a protein interactome study has determined that a majority (>60%) of the proteins interacting with TALK-1 are ER-resident proteins (26). Similarly, a human pancreatic islet cDNA library generated and screened in a membrane yeast-two-hybrid assay to identify islet TALK-1 interacting proteins detected multiple ER-resident proteins that interact with TALK-1 (27). In accordance with these observations, TALK-1 shows substantial intracellular staining in human and mouse pancreatic β-cells (28). Although these findings suggest that TALK-1 channels may serve an intracellular role, investigations of intracellular K2P channels have focused primarily on elucidating the factors that enable their functional expression on the plasma membrane, and an ER function for K2P channels has not been identified.

In β-cells, TALK-1 contributes to plasma membrane potential (V_m) hyperpolarization, thereby regulating cytosolic Ca^{2+} (Ca^{2+}_c) influx and insulin secretion (28). TALK-1 is distributed in pancreatic islets as well as gastric somatostatin cells (29, 30), and is the most abundant islet K^+ channel at the transcriptional level (31–33). A primary physiological function of β-cell TALK-1 channels is to limit glucose-induced islet electrical and Ca^{2+}_c oscillations, controlling second-phase pulsatile insulin secretion (28). Furthermore, a non-synonymous polymorphism in TALK-1 (rs1535500) associated with T2DM (34–36) causes a gain-of-function in TALK-1 activity (28), which may impair Ca^{2+}_c oscillations and pulsatile insulin secretion. However, the molecular mechanisms underlying TALK-1 regulation of islet Ca^{2+}_c oscillations remain unclear.

Here, we tested the hypothesis that TALK-1 channels were functional in the ER and mediated ER K^+ countercurrents which support β-cell Ca^{2+}_{ER} homeostasis. By measuring

Ca^{2+}_{ER}, Ca^{2+}_{c}, and single-channel K2P currents on the ER membrane, we demonstrated that TALK-1 channels conducted ER K^+ countercurrents which enhanced Ca^{2+}_{ER} leak in mouse and human β-cells. We found that TALK-1 control of β-cell Ca^{2+}_{ER} modulated islet Ca^{2+}_{c} dynamics, which has important implications for understanding the regulation of Ca^{2+}_{c} oscillations that underlie pulsatile insulin secretion. Moreover, we showed that other ER-localized K2P channels, such as TASK-1, could function in an identical manner. Inhibition of K^+ currents through either TALK-1 or TASK-1 increased steady-state Ca^{2+}_{ER} concentrations, demonstrating that the K^+ channel function of these proteins was essential for their effects on Ca^{2+}_{ER} homeostasis. Moreover, islets from mice lacking TALK-1 channels showed reduced signs of ER stress induced by chronic exposure to a high-fat diet (HFD), suggesting that defects in TALK-1 channel activity can perturb ER health and contribute to islet dysfunction in T2DM. Overall, these findings identify an intracellular function of K2P channels, and reveal TALK-1 channels as a possible therapeutic target to modulate Ca^{2+}_{ER} homeostasis to reduce β-cell ER stress in diabetes.

RESULTS

TALK-1 activity promotes Ca^{2+}_{ER} leak

TALK-1's prominent intracellular staining pattern (28) and physical association with several ER-resident proteins (26) suggested that TALK-1 could be localized to the ER. To determine the subcellular localization of TALK-1, we performed immunofluorescence staining of mouse pancreas sections, and detected co-localization of TALK-1 with the ER marker calreticulin (Fig. 1A). Additionally, co-expression of a TALK-1/mCherry fusion protein and an ER-targeted indicator (37) in mouse islet cells revealed TALK-1 in the ER (Fig. S1).

While TALK-1 conducts K^+ currents on the plasma membrane in β-cells (28), it has not yet been determined whether K2P channels in the ER, such as TALK-1, are functional. To test if TALK-1 channel function could affect Ca^{2+}_{ER} homeostasis, we first directly measured β-cell Ca^{2+}_{ER} from control (wild-type) and TALK-1 KO islets (28) with the ER-targeted, genetically encoded Ca^{2+} indicator D4ER (38) (Fig. 1B). Under both low and high glucose conditions, TALK-1 KO β-cells had significantly higher Ca^{2+}_{ER} concentrations (Fig. 1, B and C). Inhibition of sarco-endoplasmic Ca^{2+} ATPases (SERCAs) with cyclopiazonic acid (CPA) produced a greater decrease in Ca^{2+}_{ER} in KO β-cells compared with controls (Fig. 1D). Absolute Ca^{2+}_{ER} concentrations in KO β-cells remained above wild-type β-cells after application of CPA. These findings suggest that inhibition of SERCAs was insufficient to completely empty β-cell Ca^{2+}_{ER} stores, as observed in neurons (39), and implied that TALK-1 channels were a critical determinant of β-cell steady-state Ca^{2+}_{ER} concentrations. As a slight reduction in Ca^{2+}_{ER} stimulates β-cell proliferation (40), we tested if TALK-1 activity affected β-cell number or proliferation. The absence of TALK-1 did not alter islet cellular composition, nor did it impair adaptive proliferation (as determined by BrdU incorporation) in response to a short term (one week) HFD stimulus (41) (Fig. S2, A to F), suggesting that inhibition of TALK-1 did not influence islet cell composition.

To further confirm that TALK-1 modulates Ca^{2+}_{ER}, we quantified Ca^{2+}_{ER} indirectly in wild-type and KO β-cells by measuring Ca^{2+}_{c} in response to multiple stimuli. Treating β-cells with the Ca^{2+} ionophore ionomycin in the absence of extracellular Ca^{2+} resulted in more

Ca^{2+} release from KO than wild-type β-cells (Fig. S3, A and B), suggesting increased intracellular Ca^{2+} stores. We next perfused isolated wild-type and TALK-1 KO β-cells with Ca^{2+}-free buffer containing diazoxide to selectively monitor Ca^{2+}_c independently of Ca^{2+} entry through plasma membrane channels (Fig. 1E). Under these conditions, TALK-1 KO β-cells exhibited lower basal Ca^{2+}_c, and the addition of CPA produced a larger increase in Ca^{2+}_c (Fig. 1, E and F), suggesting reduced Ca^{2+}_{ER} leak and increased Ca^{2+}_{ER} stores. Following washout of CPA, addition of Ca^{2+} to the extracellular buffer led to a similar amount of Ca^{2+}_c influx in wild-type and TALK-1 KO cells, showing that activation of store-operated Ca^{2+} entry (SOCE) was not impaired in TALK-1 KO β-cells (Fig. 1, E and F). However, the reduced basal Ca^{2+}_c observed without external Ca^{2+} was maintained in the presence of extracellular Ca^{2+} in TALK-1 KO β-cells (Fig. 1, E and G).

As TALK-1 is also detected in human β-cells (28), we next examined whether TALK-1 was present in the ER of human β-cells. Immunofluorescent staining of human pancreas sections revealed co-localization of TALK-1 with the ER marker calreticulin (Fig. 2A). To assess TALK-1-mediated regulation of human β-cell Ca^{2+}_{ER}, we measured CPA-induced Ca^{2+}_{ER} release in β-cells expressing a dominant-negative TALK-1 (TALK-1 DN) construct (Fig. 2B). The TALK-1 DN contains a pore mutation which inhibits K^+ conductance when it interacts with endogenous TALK-1 (28). The TALK-1 DN construct also contains a P2A element between the sequences encoding TALK-1 and an mCherry reporter, allowing us to detect cells expressing the TALK-1 DN by mCherry fluorescence; β-cells were identified by post-staining for insulin (28). Inhibition of TALK-1 with the TALK-1 DN caused a significant increase in CPA-induced Ca^{2+}_{ER} release (Fig. 2C), demonstrating that TALK-1 modulates Ca^{2+}_{ER} homeostasis in human β-cells.

To test whether TALK-1 activity reduced Ca^{2+}_{ER} storage, we examined the effects of TALK-1 expression on Ca^{2+}_{ER} in HEK293 cells. Two channel-forming isoforms of TALK-1 (1b and 1a) (42) co-localized with an ER-targeted YFP marker in these cells (Fig. 3A). We next assessed the consequences of TALK-1 expression on Ca^{2+}_{ER} homeostasis in these cells. To minimize potential deleterious effects of protein overexpression, we used the TALK-1 DN mutant as a control, which permitted dissociation of the effects of TALK-1-mediated K^+ conductance and protein-protein interactions on Ca^{2+}_{ER} homeostasis. Overexpression of K^+-conducting wild-type TALK-1 yielded a substantial increase in basal Ca^{2+}_c and a concomitant reduction in total Ca^{2+} released from the ER during CPA-induced inhibition of SERCAs when compared to the non-K^+-conducting TALK-1 DN channels (Fig. 3, B through D). These observations suggest that TALK-1 channel activity promotes Ca^{2+}_{ER} leak. Addition of Ca^{2+} to the extracellular buffer produced a larger increase in Ca^{2+}_c in wild-type-TALK-1 compared to TALK-1 DN-expressing cells, and similar to CPA-induced Ca^{2+}_{ER} release, stimulation of IP3-triggered Ca^{2+}_{ER} release with carbachol elicited a greater response in cells expressing TALK-1 DN (Fig. 3, B and E). Thus, the K^+-channel function of TALK-1 is sufficient to alter Ca^{2+}_{ER} homeostasis.

To confirm the specificity of the effect of TALK-1 on Ca^{2+}_{ER}, we compared Ca^{2+}_{ER} storage in cells stably and inducibly expressing different K2P channels (43) (Fig. 4A, Fig. S4, A and B). Similar to transfected cells, TALK-1 induction reduced Ca^{2+}_{ER} stores (Fig. 4A). We also found that expression of TASK-1 (Fig. 4A) and TASK-3 (Fig. S5, A and B) channels (21,

22) also caused a reduction in Ca^{2+}_{ER}. We confirmed the Ca^{2+}_{ER} reduction in TALK-1- and TASK-1-expressing cells by directly measuring Ca^{2+}_{ER} using the genetically encoded Ca^{2+}_{ER} indicator T1ER (44) (Fig. 4B). However, not all K2P channels influenced Ca^{2+}_{ER}, as demonstrated by the absence of a Ca^{2+}_{ER} phenotype following induction of TREK-2 or TREK-1 channels (Fig. 4A, Fig. S5 C through F).

This finding prompted us to examine whether pharmacological modulation of K2P channels could be used to manipulate Ca^{2+}_{ER} storage. Because specific pharmacology for TALK-1 channels does not presently exist, we tested if selective TASK-1 inhibition with ML365 (a small molecule antagonist of TASK-1 (45), and a partial TASK-3 inhibitor) could influence Ca^{2+}_{ER}. Inhibition of TASK-1 channel activity with ML365 treatment significantly restored Ca^{2+}_{ER} loss caused by TASK-1 channel induction (Fig. 4, C and D). As ML365 also partially blocks TASK-3, treatment of TASK-3-expressing cells with this compound caused a modest increase in Ca^{2+}_{ER} (Fig. S5, A and B). However, ML365 did not influence Ca^{2+}_{ER} in cells expressing TREK-1 or TREK-2 (Fig. S5, C through F). These data further support the hypothesis that K^+ flux through ER K2P channels enhances Ca^{2+}_{ER} leak.

Although these observations suggested that pharmacological modulation of K2P channels could be used to regulate Ca^{2+}_{ER}, immortalized cell lines expressing TASK-1 may not recapitulate Ca^{2+}_{ER} handling of primary tissues. Thus, we tested whether pharmacological blockade of TASK-1 could alter Ca^{2+}_{ER} in primary islet α-cells, where they regulate glucagon secretion (46). ML365 treatment increased α-cell Ca^{2+}_{ER} stores (Fig. 4, E and F). These data demonstrate that TASK-1 affects α-cell Ca^{2+}_{ER} homeostasis, and that pharmacological inhibition of Ca^{2+}_{ER}-modulating K2P channels could be used to control Ca^{2+}_{ER} in primary islet cells.

TASK-1 mutations have been implicated in pulmonary arterial hypertension (PAH), one of which (G203D) is a dominant-negative mutation that directly impairs K^+ conductance through TASK-1 (47). Expression of TASK-1 G203D produced a significantly greater increase in Ca^{2+}_{ER} stores compared to that of control TASK-1 channels (Fig. S5, G and H), an effect similar to that of expressing the TALK-1 DN mutant, which increased Ca^{2+}_{ER} stores compared to cells expressing wild-type TALK-1. These observations imply that defects in TASK-1 K^+ conductance may inappropriately increase Ca^{2+}_{ER} or impair physiologically important Ca^{2+}_{ER} fluxes.

TALK-1 and TASK-1 form functional channels across the ER membrane

During Ca^{2+}_{ER} release, K^+ moves across the ER membrane to maintain ER electroneutrality and sustain the driving force for Ca^{2+}_{ER} release (14, 16, 48, 49). To directly assess whether TALK-1 functions as an ER K^+ channel, we used nuclear patch clamp electrophysiology (50) to measure channel activity on the outer nuclear membrane, which is continuous with the ER (Fig. 5, A and B). In nuclei from cells expressing TREK-2, which does not affect Ca^{2+}_{ER}, we did not detect TREK-2 channel activity (Figure 5C). However, nuclei from cells expressing TALK-1 (Fig. 5D) or TASK-1 (Fig. 5E) exhibited single-channel openings consistent with their respective biophysical profiles, suggesting that TALK-1 and TASK-1 form functional channels on the ER membrane.

These results implied that TALK-1 and TASK-1 regulate Ca^{2+}_{ER} homeostasis by allowing K^+ flux across the ER membrane. We further tested whether TALK-1 modulation of Ca^{2+}_{ER} release depended on K^+ flux by manipulating the cytosolic K^+ concentration. Using digitonin-permeabilized HEK293 cells expressing wild-type or DN TALK-1 and the genetically encoded Ca^{2+}_{ER} indicator G-CEPIA1er (37), we examined Ca^{2+}_{ER} leak in response to SERCA inhibition with CPA. In the presence of K^+, Ca^{2+}_{ER} leak was faster in cells expressing wild-type TALK-1 compared to TALK-1 DN (Fig. S6, A through D). Therefore, K^+ flux through TALK-1 supports the movement of Ca^{2+} across the ER membrane. We also examined whether TALK-1 functions as an ER K^+ channel in primary cells by performing nuclear patch clamp recordings on nuclei isolated from wild-type and TALK-1 KO islets. We detected single channel openings (Fig. 5F) with a current amplitude comparable to cloned TALK-1 in 55.6 ±6.3% of wild-type islet cell nuclei (Fig. 5G). However, only 31.2 ±2.7% of nuclei from TALK-1 KO islets displayed K2P-like channel openings (Fig. 5H). Together, our findings suggest that TALK-1 and TASK-1 form functional channels on the ER membrane, allowing for a K^+ countercurrent that supports Ca^{2+}_{ER} leak and helps to set Ca^{2+}_{ER}.

TALK-1 regulation of β-cell Ca^{2+}_{ER} handling modulates islet Ca^{2+} oscillations

To dissect the role of TALK-1 modulation of Ca^{2+}_{ER} during β-cell Ca^{2+} influx, we controlled β-cell Ca^{2+}_{c} influx with K^+-induced depolarization of diazoxide-treated cells, in the presence or absence of the SERCA inhibitor thapsigargin (51) (Fig. 6A). Under these conditions, the role of plasma membrane TALK-1 channels is effectively dissociated from its intracellular functions: diazoxide circumvents the depolarizing effects of glucose by activating K_{ATP} channels, and K^+ depolarization activates voltage-gated Ca^{2+} channels (VDCCs) independently of K^+ channel activity (52). Subtracting the control trace from the thapsigargin-treated trace revealed the Ca^{2+}_{ER} contribution to the Ca^{2+}_{c} signal (Fig. 6B). During Ca^{2+} influx, Ca^{2+}_{ER} uptake was observed (Figure 6B, downward deflection), whereas Ca^{2+}_{ER} release occurred following the depolarizing K^+ pulse (Figure 6B, upward component). We found reduced Ca^{2+}_{ER} release in KO β-cells (Fig. 6, B and C), in accordance with our finding that TALK-1 channel activity promotes Ca^{2+}_{ER} release.

β-cell Ca^{2+}_{ER} release has been implicated in the activation of hyperpolarizing Ca^{2+}-activated K^+ currents (53–55). When stimulated with glucose, KO islets show accelerated Ca^{2+} oscillations (28), which may be due to changes in Ca^{2+}_{ER} control of the V_m and VDCC activity. We tested this by depleting Ca^{2+}_{ER} using CPA in wild-type and TALK-1 KO islets undergoing glucose-stimulated Ca^{2+} oscillations (Fig. 6D). Under low glucose conditions, basal Ca^{2+}_{c} concentrations were modestly lower in KO islets (Fig. 6E). Upon stimulation with high glucose, Ca^{2+} influx was significantly greater in KO islets (Fig. 6E). However, Ca^{2+}_{ER} depletion with CPA normalized Ca^{2+}_{c} concentrations in KO islets to similar to those in wild-type islets (Fig. 6E). As depletion of Ca^{2+}_{ER} removes the contribution of the ER from the glucose-stimulated Ca^{2+}_{c} signal, this finding suggested that TALK-1 influences β-cell Ca^{2+}_{c} by modulating Ca^{2+}_{ER} handling, which in turn regulates plasma membrane K^+ currents and Ca^{2+} influx. Therefore, we proceeded to test the relationship between TALK-1 regulation of Ca^{2+}_{ER} release and β-cell Ca^{2+}-activated K^+ currents.

The termination of each electrical oscillation is triggered by a slowly activating, Ca^{2+}-dependent K^+ current termed K_{slow}, which is mediated by intermediate-conductance K_{Ca} channels (IK), apamin-insensitive small conductance (SK) K_{Ca} channels, and K_{ATP} channels (55–57). The β-cell ER can release Ca^{2+} close to the plasma membrane (58), and K_{slow} activity is sensitive to Ca^{2+}_{ER} release (53–55). In KO islets, V_m repolarization is reduced by approximately 50% at the termination of each electrical oscillation (28), suggesting that K_{slow} may be impaired in KO islets. We tested this notion by measuring K_{slow} in wild-type and KO β-cells. K_{slow} amplitude (Fig. 7A, inset) was reduced in KO β-cells by 48 ±17% relative to wild-type β-cells (Fig. 7, B and C). TALK-1 is not activated by Ca^{2+}_c in oocytes (59), and we also found that TALK-1 activity in HEK293 (Fig. 7D) or β-cells (Fig. 7E) was insensitive to Ca^{2+}_c, making it unlikely that TALK-1 is a constituent channel of K_{slow}. These findings suggest that TALK-1 may modulate β-cell K_{slow} indirectly through control of Ca^{2+}_{ER} homeostasis. To assess whether modulation of K2P channels activity affects depolarization-induced Ca^{2+}_{ER} uptake and release, we inhibited TASK-1 in α-cells with ML365. We found that TASK-1 channel inhibition reduced Ca^{2+}_{ER} release induced by V_m depolarization (51) (Fig. 7, G and H), suggesting that TASK-1 facilitates α-cell Ca^{2+}_{ER} release.

TALK-1 channel activity exacerbates islet ER stress

Reduced β-cell Ca^{2+}_{ER} content is associated with ER stress and islet dysfunction in diabetes (4, 60–63). Our results indicated that TALK-1 channels were a determinant of β-cell Ca^{2+}_{ER} concentrations, and suggested that TALK-1 channel activity could exacerbate Ca^{2+}_{ER} depletion which leads to ER stress. Therefore, we determined whether the absence of functional TALK-1 channels impacted islet responses to the metabolic stress of a HFD. After one week of HFD feeding, the expression of genes involved in ER stress signaling did not differ between wild-type and TALK-1 KO islets (Fig. 8A). SERCA abundance is reported to change as a function of Ca^{2+}_{ER} content (64, 65); however, we did not detect differences in the expression of mRNAs encoding SERCA2b and SERCA3 in wild-type and TALK-1 KO islets. However, after prolonged (20 weeks) exposure to a HFD, TALK-1 KO islets exhibited decreased expression of multiple ER stress genes, as well as significantly decreased expression of mRNA encoding SERCA2b and SERCA3 (Fig. 8B). The decreased *SERCA* expression may represent a compensatory mechanism to reduce Ca^{2+}_{ER} overloading and maintain β-cell Ca^{2+}_{ER} concentrations in an optimal range.

We also assessed whether the T2DM-linked gain-of-function polymorphism (rs1535500) encoding TALK-1 A277E (28) interfered with ER function. ATF6 transcriptional activation occurs in response to ER Ca^{2+} depletion and protein misfolding (65, 66), which we measured in INS-1 cells (with a luciferase reporter containing five tandem repeats of ATF6 binding sites (67, 68)) after application of tunicamycin, which inhibits protein glycosylation and causes protein misfolding and ER stress. INS-1 cells expressing wild-type TALK-1 or TALK-1 A277E were significantly more susceptible to tunicamycin-induced ATF6 activation than cells expressing the non-conducting TALK-1 DN. Furthermore, TALK-1 A277E activated ATF6 to a significantly greater extent than wild-type TALK-1 (Fig. 8C). However, co-expression of TALK-1 A277E with the TALK-1 DN reduced ATF6 activation to amounts comparable to that induced by expression of TALK-1 DN alone (Fig. 8C). INS-1

cells expressing TALK-1 A277E showed reduced Ca^{2+}_{ER} concentrations compared to cells expressing wild-type TALK-1 (Fig. 8D). Together, our findings indicate that TALK-1 channels control Ca^{2+}_{ER} fluxes in the islet, which may regulate plasma membrane ion channel activity, electrical excitability, and Ca^{2+}_{ER} concentrations important for protein processing (Fig. S7).

DISCUSSION

Tight regulation of β-cell Ca^{2+}_{ER} is required to sustain insulin synthesis, metabolism, as well as intracellular Ca^{2+} signaling, and perturbations in Ca^{2+}_{ER} handling contribute to diabetes pathogenesis. β-cell Ca^{2+}_{ER} is controlled by several proteins including SERCAs (38, 62), IP3Rs (69), RyRs (2, 69, 70), and the translocon (71). However, the ubiquitous distribution of most Ca^{2+}_{ER} handling proteins precludes their clinical use in treating diabetes. Here, we demonstrated that pharmacological manipulation of K2P channels can be used to control primary cell Ca^{2+}_{ER}. Moreover, our data indicated that inhibiting TALK-1 channel activity could protect islets from ER stress induced by prolonged exposure to a HFD. These observations suggest the exciting potential of utilizing K2P channels such as TALK-1 as a therapeutic target to reduce β-cell ER dysfunction under diabetic conditions.

Ca^{2+}_{ER} is determined by a balance of SERCA activity, Ca^{2+}_{ER} release, and Ca^{2+}_{ER} buffering. Ca^{2+}_{ER} release shifts the ER membrane potential ($V_{m(ER)}$) towards the Ca^{2+}_{ER} reversal potential ($E_{Ca^{2+}(ER)}$), where net Ca^{2+}_{ER} efflux would stop. However, the K^+ countercurrent across the ER membrane maintains $V_{m(ER)}$ positive of $E_{Ca^{2+}(ER)}$, facilitating Ca^{2+}_{ER} release (16, 20, 49, 72). Our data indicate that ER TALK-1 K^+ currents support the electrochemical driving force for Ca^{2+}_{ER} release, consistent with our observation that TALK-1 overexpression decreased Ca^{2+}_{ER} storage by increasing Ca^{2+}_{ER} leak. Conversely, inhibition of TALK-1 should move the $V_{m(ER)}$ closer to $E_{Ca^{2+}(ER)}$, resulting in reduced Ca^{2+}_{ER} leak and increased Ca^{2+}_{ER} (15), a prediction in accordance with the phenotype of TALK-1 KO β-cells.

Although a diminished contribution of Ca^{2+}_{ER} leak to bulk Ca^{2+}_{c} might be predicted to impair GSIS, TALK-1 KO islets exhibit increased glucose-stimulated Ca^{2+} influx and insulin secretion (28). These observations suggest that β-cell Ca^{2+} influx through VDCCs is increased following loss of TALK-1 channels. Ca^{2+}_{ER} can play important roles in controlling plasma membrane channels that tune VDCC activity. For example, β-cell Ca^{2+}_{ER} release influences insulin secretion through modulation of currents which hyperpolarize the V_m, such as K_{slow}, thereby indirectly controlling VDCC activity. In TALK-1 KO β-cells, reduced Ca^{2+}_{ER} release presumably results in less K_{slow} activation, leading to V_m depolarization and more persistent electrical activity, culminating in a net increase in Ca^{2+}_{c} and enhanced GSIS. Ca^{2+}_{ER} release serves an important role in regulating 2^{nd}-phase Ca^{2+}_{c} influx and insulin secretion, which are increased when SERCAs are inhibited pharmacologically and is also observed in islets lacking SERCA3 (38, 73, 74). Similarly, we find that both 2^{nd}-phase Ca^{2+}_{c} and insulin secretion are increased in the absence of functional TALK-1 channels (28). These observations suggest that TALK-1 modulation of the Ca^{2+}_{ER} handling which control 2^{nd}-phase insulin secretion is a key physiological function of β-cell TALK-1 channels.

As mentioned above, TALK-1 KO islets exhibit increased insulin secretion, a higher frequency of Ca^{2+}_c oscillations, and increased plateau fraction (the fraction of time spent in electrically excitable periods) (28). The present study helps resolve the molecular mechanisms underlying these phenotypes. A rationale for the increased plateau fraction and oscillation frequency in TALK-1 KO islets is that ER TALK-1 channels sustain Ca^{2+}_{ER} release, which results in greater K_{slow} activity and V_m hyperpolarization. Because this Ca^{2+}_{ER} release is reduced in TALK-1 KO β-cells, K_{slow} activation is diminished, resulting in an increased plateau fraction. This is in accordance with observations that depletion of Ca^{2+}_{ER} inhibits K_{slow} and accelerates Ca^{2+}_c oscillations (53). Ca^{2+}_{ER} concentrations also determine the activation of depolarizing store-operated currents, as demonstrated by the acceleration of V_m and Ca^{2+}_c oscillations after treatment of islets with SERCA inhibitors (75–77), presumably due to inhibition of K_{slow} and activation of SOCE. These observations highlight that SOCE serves an important role in shaping islet Ca^{2+}_c oscillations, and future studies are required to dissect the relationship between TALK-1 modulation of Ca^{2+}_{ER} stores, SOCE, V_m and Ca^{2+}_c oscillations, and insulin secretion.

ER K^+ channels are also important for Ca^{2+}_{ER} uptake, as demonstrated by the influence of ER-localized SK channels in regulating neuronal and cardiomyocyte ER and SR Ca^{2+} uptake (20). SK channels are predicted to preserve ER pH homeostasis through activation of an ER K^+/H^+ antiporter that promotes ER H^+ entry to balance SERCA-mediated H^+ loss during Ca^{2+} uptake (20). Although we cannot exclude a role for K2P channels in modulating SERCA function, we found reduced basal Ca^{2+}_{ER} when TALK-1 was heterologously expressed, and conversely found increased Ca^{2+}_{ER} in TALK-1 KO β-cells. These findings suggest that if TALK-1 controls Ca^{2+}_{ER} uptake, it would presumably do so by inhibiting SERCA function, in contrast to SK channels, which enhance SERCA function. Any effects of TALK-1 on SERCA activity could be through indirect mechanisms modulated by Ca^{2+}_{ER}, such as mitochondrial ATP production which energizes the β-cell SERCA pump (78).

Our observations suggested that TALK-1 activity controls Ca^{2+}_{ER}, which impacts many aspects of β-cell function in health and disease. In addition to controlling Ca^{2+}_c signals, another essential function of β-cell Ca^{2+}_{ER} handling is to maintain insulin production and processing, which is impaired under conditions of β-cell stress induced by insulin resistance or decreased β-cell mass. A hallmark of ER stress is increased Ca^{2+}_{ER} leak (2), which can be caused in β-cells by reductions in the abundance of proteins which affect Ca^{2+}_{ER} such as SERCA2b (60, 62) or sorcin (68). Our data indicate that TALK-1 activity aggravated islet ER stress under conditions of increased systemic insulin demand. Moreover, our finding that T2DM-associated TALK-1 A277E channels exacerbated Ca^{2+}_{ER} leak and ER stress responses suggests that defects in TALK-1 channel activity could contribute to islet ER dysfunction in diabetes. *TALK-1* transcript abundance is reduced under conditions that cause ER stress in diabetes (such as palmitate or inflammatory cytokine treatment (79)), which may be a protective mechanism to preserve β-cell Ca^{2+}_{ER} homeostasis by reducing Ca^{2+}_{ER} leak. It will be important to determine how TALK-1 participates in the cellular response to other diabetes-associated ER stressors.

Mutations in other K2P channels have also been associated with various disorders that may be associated with defects in Ca^{2+}_{ER} handling. For example, dominant-negative mutations in

TASK-1 or TASK-3 result in PAH or Birk-Barel syndrome, respectively (47). We found that a PAH-linked mutation in TASK-1 (G203D) enhanced Ca^{2+}_{ER} stores relative to wild-type TASK-1. Thus, in patients with the TASK-1 G203D mutation, disruptions in ER/SR Ca^{2+} handling may contribute to PAH (80). In pulmonary arterial smooth muscle cells, impaired Ca^{2+}_{ER} transfer to mitochondria leads to pulmonary vascular remodeling, a defect that can be targeted with clinically used chemical chaperones to ameliorate PAH (80, 81). Inhibition of TASK-1 using the specific inhibitor A293 causes pulmonary vascular remodeling and PAH in rats, and pharmacological activation of TASK-1 protects from the development of PAH (82). TASK-3 also controls Ca^{2+}_{ER}, and a mutation in *KCNK9* (which encodes TASK-3, G236R) causes Birk-Barel syndrome, which is characterized by intellectual disability, hypotonia, and facial dysmorphism. TASK-3 is also implicated in mitochondrial function (83), highlighting the importance of determining the relationship between TASK-3 modulation of Ca^{2+}_{ER} handling and mitochondrial function. As we found that pharmacological regulation of TASK-1 could control primary cell Ca^{2+}_{ER}, K2P channels such as TASK-1, TASK-3 or TALK-1 could be targeted for cell-selective therapies to reduce ER dysfunction.

Not all K2P channels regulate Ca^{2+}_{ER}, as demonstrated by our finding that neither TREK-1 channels nor TREK-2 channels affected Ca^{2+}_{ER} homeostasis. These findings could be due to localization of these channels; TREK-1 channels are found primarily on the plasma membrane (84), whereas the subcellular localization of TREK-2 channels has not been determined. However, all K^+ channels are assembled in the ER prior to their delivery to the plasma membrane (85). It remains to be determined how certain K2P channels (specifically, TALK-1, TASK-1, and TASK-3) regulate Ca^{2+}_{ER} whereas others (specifically, TREK-1 and TREK-2) do not. As many K^+ channels, such as K_{ATP}, require a physical interaction with the plasma membrane lipid phosphatidylinositol 4,5-bisphosphate (PIP_2) to conduct K^+, K2P channels that are dependent on PIP_2 for activity may not function in the ER membrane. This property could be due to intrinsically low PIP_2 concentrations on the ER membrane, which limits K^+ channel activity until they are transported to the plasma membrane (86). TREK-1 is highly sensitive to PIP_2, whereas both TASK-1 and TASK-3 channels, both of which affect Ca^{2+}_{ER}, are insensitive to PIP_2 (87). Future studies are needed to better understand the regulatory mechanisms underlying K2P channel activity in the ER, and how these impact Ca^{2+}_{ER} homeostasis.

In conclusion, we demonstrate that TALK-1 in the ER regulates Ca^{2+}_{ER} handling, thus controlling K_{slow} activity, Ca^{2+} influx, and insulin secretion. These findings highlight a physiological function of K2P channels in the regulation of Ca^{2+}_{ER}. K2P channels may provide cell-selective targets to modulate Ca^{2+}_{ER} to treat the many diseases characterized by dysfunctional Ca^{2+}_{ER} handling.

MATERIALS AND METHODS

Chemicals

Unless otherwise specified, all reagents were obtained from Sigma-Aldrich.

Mouse Models

The mice used in this study were 8–12 week-old males on a C57Bl6/J background. The generation of *Kcnk16*$^{-/-}$ (TALK-1 KO) mice has been previously described (28). For experiments using mouse α-cells, transgenic mice expressing tdRFP specifically in α-cells were used (46). All mice used in this study were handled in compliance with protocols reviewed and approved by the Vanderbilt University Institutional Animal Care and Use Committee, according to guidelines set forth by the NIH.

Islet isolation and culture

Mouse islets were isolated using collagenase P (Roche) digestion of the pancreas and density gradient centrifugation (5). Human islets from adult nondiabetic donors (donor information is provided in Table S1) were obtained through isolation centers organized by the Integrated Islet Distribution Program. In experiments using D4ER, cells were transduced with Ad-D4ER (38) 48 hours prior to imaging. In human β-cell experiments, cells were transfected with TALK-1 DN- or mCherry-expressing plasmids (28). Islets and dispersed cells were cultured for 24–48 hours prior to experimentation (28).

Cell culture and luciferase assays

The development of TREx-293 cells with inducible expression of K2P channels has been previously described (43). To measure TALK-1 and TASK-1 expression in induced cells, lysates from TALK-1- or TASK-1-TREx-293 cells treated for 24 hours with or without tetracycline (1 μg/mL) induction were run on 4−12% Bis-Tris polyacrylamide gels (Invitrogen). The protein was then transferred to a nitrocellulose blotting membrane (BioRad) which was probed with TALK-1 (Novus Biologicals #NBP1-83071) or TASK-1 (Abcam #49433) antibodies. Equal loading of wells was assessed by stripping and reprobing membranes with a β-actin antibody (Cell Signaling Technologies #4970). Representative blots are shown in Fig. S4. For experiments comparing the effects of wild-type TALK-1 and TALK-1 DN on Ca^{2+}_{ER} handling, HEK293 cells were transfected with pCDNA3.1 plasmids encoding these channels using Lipofectamine 3000 (Thermo Fisher) according to the manufacturer's instructions, and imaged 48 hours post-transfection.

INS-1 (832/13) cells were cultured in RPMI 1640 supplemented with 15% FBS and penicillin-streptomycin. INS-1 cells were transfected with p5×ATF6-GL3 (Addgene #11976) and plasmids encoding wild-type TALK-1, TALK-1 A277E, or TALK-1 DN (28). Cells were incubated overnight with vehicle (DMSO) or tunicamycin (0.25 μg/mL) for 16–20 hours prior to performing a luciferase assay using the Steady-Glo Luciferase Assay System (Promega) according to the manufacturer's instructions.

Patch clamp electrophysiology

An Axopatch 200B amplifier (Molecular Devices) was used to measure whole-cell K^+ channel currents in the voltage-clamp mode; currents were digitized using a Digidata 1440, lowpass filtered at 1 kHz and sampled at 10 kHz. For K_{slow} recordings, pipettes were filled with an intracellular solution (57) containing (in mM) 28.4 K_2SO_4, 63.7 KCl, 11.8 NaCl, 1 $MgCl_2$, 20.8 HEPES, 0.5 EGTA (pH 7.22 with KOH) and ~0.05 mg·ml^{-1} amphotericin B. Nuclear patch clamp experiments were preformed using the approach described by Mak and

colleagues (50). Nuclei were patched in a solution containing (in mM): 150 KCl, 10 HEPES, 0.5 EGTA, 0.36 $CaCl_2$ (pH 7.3 with KOH). Patch electrodes were pulled to a resistance of 8–10 MΩ, loaded with recording solution, and coated with Sigmacote. Single-channel currents were lowpass filtered at 1 kHz and sampled at 50 kHz. When intracellular [Ca^{2+}] was clamped, cells were recorded using the whole-cell configuration using electrodes filled with a solution containing (in mM) 140 KCl, 5 HEPES, 4 Mg·ATP, 1 EGTA, 137 μM (for 50 nM Ca^{2+} final) or 946 μM (for 5 μM Ca^{2+} final) $CaCl_2$, (pH 7.22 with KOH). [Ca^{2+}] was determined using MAXCHELATOR software. The extracellular buffer used for islet-cells (A modified Krebs-Ringer buffer, KRB) contained (in mM) 119 NaCl, 2.5 $CaCl_2$, 4.7 KCl, 25 HEPES, 1.2 $MgSO_4$, 1.2 KH_2PO_4, 11 glucose (pH 7.35 with NaOH). The extracellular buffer used for HEK293 cells (HEK buffer) contained (in mM) 150 NaCl, 5 KCl, 2 $MgCl_2$, 2.5 $CaCl_2$, 10 HEPES, and 10 glucose (pH 7.35 with NaOH). When assessing the Ca^{2+} sensitivity of TALK-1 in β-cells, the extracellular buffer was supplemented with a cocktail of K^+ channel inhibitors including 200 μM tolbutamide (MP Biomedicals), 10 mM tetraethylammonium chloride (Acros Organics), 100 nM apamin (Alomone Labs), 100 nM iberiotoxin (Alomone Labs), 100 nM TRAM-34 (Alomone Labs), and 10 μM nifedipine to inhibit voltage-gated Ca^{2+} channels. Cells were recorded with a voltage-clamp protocol used to assess K2P channel currents (28). Recordings were analyzed using Clampfit 10 (Molecular Devices) and Microsoft Excel software.

Calcium imaging

Mouse and human β-cells were loaded with 2 μM Fura-2 AM (Molecular Probes) and imaged as previously described (88). Cyclopiazonic acid (CPA; Alomone Labs) was used at a concentration of 50 μM; ionomycin was used at a concentration of 5 μM (Alomone Labs). Human β-cells were post-stained for insulin (88). In all experiments, cells were perfused with a flow of 2 $mL \cdot min^{-1}$ at 37 °C. For analysis of mouse β-cell Ca^{2+}_{ER} uptake and release (51), Fura-2 loaded cells were incubated for 10 minutes in KRB supplemented with 11 mM glucose, 125 μM diazoxide (Enzo) and 1.25 μM thapsigargin (Alomone Labs) or vehicle. In high-[K^+] stimulus buffer, NaCl was reduced accordingly to maintain osmolarity. For experiments using D4ER, cells were incubated for 20 minutes in KRB containing 2 mM glucose prior to imaging.

For assays comparing the effects of expression of K2P channels in stably transduced TREx-293 cells, 30,000 cells/well were seeded to 384-well black-wall, clear-bottom, amine-coated plates (BD Biosciences). Channel expression was induced with 1 $\mu g \cdot ml^{-1}$ tetracycline in culture medium, and the cells were cultured overnight in a 5% CO_2 incubator at 37 °C. The cells were washed using an ELx405CW plate washer (Bio-Tek Instruments, Inc.), and loaded with 4 μM Fluo-4 AM (Molecular Probes) for 45 minutes in a 5% CO_2 incubator at 37 °C. The cells were then washed with buffer supplemented with 1 mM EGTA and incubated in a 5% CO_2 incubator at 37 °C for 8 minutes before imaging. Plates were then loaded into a whole-plate kinetic-imaging Functional Drug Screening System (FDSS 6000, Hamamatsu, Bridgewater, NJ) and imaged at 37 °C as previously described (43).

When assessing the effects of TASK-1 or TASK-3 channel blockade, cells were loaded three hours before imaging with 500 nM ML365 (Tocris) or DMSO vehicle in culture medium,

and in α-cells, the culture medium also contained 125 μM diazoxide. ML365 was present throughout the experiment. For high-speed imaging of α-cell Ca^{2+} influx, cells were loaded with 5 μM Fluo-4 AM for 25 minutes, followed by washing with KRB (11 mM glucose). α-cells were then patched according to the perforated patch clamp protocol described above on a Nikon Eclipse TE2000-U microscope equipped with an X-Cite 120Q widefield fluorescence light source (Excelitas Technologies) and a D-104 microscope photometer (Photon Technologies Inc.). Upon obtaining a low-leak, GΩ seal, the fluorescence light source was activated, and plasma membrane currents were recorded using the K_{slow} voltage-clamp protocol (57) simultaneously with Fluo-4 fluorescence. Currents and photometer signal were digitized and sampled at 10 kHz. For analysis of the effects of TALK-1 on the CPA-induced $Ca^{2+}{}_{ER}$ leak rate, TREx-293 cells transfected with wild-type TALK-1 or DN and CEPIA1-ER (37) (Addgene #58215) were permeabilized for 4 minutes in a 5% CO_2 incubator at 37 °C in an intracellular buffer containing (in mM): 140 potassium gluconate or 140 Tris base (K^+-free), 10 HEPES, 1 EGTA, 0.432 $CaCl_2$, 3 Mg·ATP, with sucrose added as needed to match osmolarity (pH 7.24), and supplemented with 50 $\mu g \cdot ml^{-1}$ digitonin (Santa Cruz). Cells were then washed for an additional 5 minutes in the appropriate buffer without digitonin prior to the start of imaging. To determine the rate constant of CPA-induced Ca^{2+} leak, the normalized data was fit to a one-phase exponential decay model using GraphPad Prism7 software. Data were analyzed using Nikon Elements, Microsoft Excel, Clampfit 10 and GraphPad Prism7 software.

Site-directed mutagenesis

The TASK-1 G203D point mutation was generated using a previously described approach (28). The sequences of oligonucleotide primers (Integrated DNA Technologies) used to create the TASK-1 G203D mutant were ACCACCATCGGCTTCGACGACTACGTGGCGCTGCAGA (forward) and TCTGCAGCGCCACGTAGTCGTCGAAGCCGATGGTGGT (reverse). PCRs were performed in 50 μL with Q5 high-fidelity DNA polymerase (New England Biolabs) with 100 ng of pCDNA3.1-KCNK3 plasmid. DNA was then incubated with 1 μL DpnI for two hours at 37 °C. Clones were sequenced to confirm mutagenesis.

Quantitative real-time PCR (qPCR)

qPCR of cDNA obtained from mouse islets was performed according to the approach described by Tong and colleagues (62). A list of primers can be found in Table S3.

Immunofluorescence

Processing and staining of paraffin-embedded mouse and human pancreas sections was performed as previously described (human donor information is provided in Table S2) (28). Sections were stained using primary antibodies against TALK-1 (Novus Biologicals #NBP1-83071; 1:175) and calreticulin (Santa Cruz #N-19; 1:125); secondary antibodies used were Alexa Fluor 488-conjugated donkey anti-rabbit (Jackson Immunoresearch #711-546-152; 1:300) and DyLight 650-conjugated donkey anti-goat (Thermo Fisher #SA5-10089; 1:250). HEK293 cells co-transfected with TALK-1a or TALK-1b (28) and ER-targeted EYFP (Addgene #56589) were washed twice with cold phosphate-buffered saline (PBS), then fixed in 4% paraformaldehyde (Electron Microscopy Sciences) for 30 minutes at

4 °C. Cells were then incubated in PBS supplemented with 0.2% bovine serum albumin (BSA), 2% normal donkey serum (NDS; Jackson Immunoresearch), and 0.05% Triton X-100 for one hour, followed by incubation in PBS containing primary antibodies against TALK-1 (1:175) and GFP (Novus Biologicals NB600-597; 1:300), 0.2% BSA, 1% NDS, and 0.1% Triton X-100, overnight at 4 °C. Following removal of the primary antibody solution, the cells were subjected to two 10-minute PBS washes, then incubated in the dark for one hour at room temperature in PBS containing 1% NDS and secondary antibodies: Alexa Fluor 488-conjugated donkey anti-rabbit (1:300) and Alexa Fluor 647-conjugated goat anti-mouse (Thermo Fisher A21237; 1:300). The secondary antibody solution was removed and the cells were subjected to three 8-minute PBS washes prior to imaging. All images were obtained using a Zeiss LSM 710 or Zeiss LSM 780 confocal laser scanning microscope. Images were analyzed using ImageJ software.

For analysis of islet cell numbers, paraffin embedded were processed as described above, and stained using primary antibodies against insulin (Dako #A0564; 1:500), somatostatin (Santa Cruz Biotechnology sc-7819: 1:250), and glucagon (Proteintech #15954-I-AP: 1:500); secondary antibodies used were Alexa Fluor 488-conjugated donkey anti-rabbit (Jackson Immunoresearch #711-546-152; 1:500), DyLight 650-conjugated donkey anti-goat (Thermo Fisher #SA5-10089; 1:250), Cy3-conjugated donkey anti-guinea pig (Jackson Immunoresearch #706-165-148; 1:500).

For analysis of high-fat diet induced islet-cell proliferation, age-matched wild-type and TALK-1 KO were placed on a high-fat diet (60% kcal/fat; Research Diets #D12492) for 10 days. Four days prior to sacrifice, mice were provided with drinking water containing BrdU (0.8 $mg \cdot ml^{-1}$) supplemented with Splenda artificial sweetener (20 $mg \cdot ml^{-1}$). Paraffin embedded pancreata were processed as described above, and were subjected to antigen retrieval performed in 1× NaCitrate pH 6.0, for 14 minutes in a microwave at high power, followed by cooling at room temperature in 1× NaCitrate solution for 25 minutes. Following antigen retrieval, slides were washed for 10 minutes in ddH_2O, followed by two 2-minute washes in PBS. Sections were the stained using primary antibodies against insulin (Dako #A0564; 1:500), somatostatin (Santa Cruz Biotechnology sc-7819: 1:250), glucagon (Proteintech #15954-I-AP; 1:500), and BrdU (Developmental Studies Hybridoma Bank #G3G4; 1:50). Secondary antibodies used were Alexa Flour 647-conjugated goat anti-mouse (Life Technologies #A21237: 1:250), DyLight 488-conjugated Donkey anti-mouse (Thermo Scientific #SA5-10166; 1:300), and Alexa Flour 594-conjugated Donkey Anti-Guinea Pig (Jackson Immunoresearch #706-586-148; 1:400), DyLight 650-conjugated donkey anti-goat (Thermo Fisher #SA5-10089; 1:250), Alexa Fluor 488-conjugated donkey anti-rabbit (Jackson Immunoresearch #711-546-152; 1:500). Blocking was done in a dark humidity chamber for one hour using Dako Blocking Solution (Ref # X0909). Primary antibodies were diluted to above concentrations in DAKO Antibody Diluent Solution (Ref#S3002) and incubated on the sections overnight at 4 °C. Following primary antibody incubation, slides were washed for 5 minutes in PBS twice. Secondary antibodies were diluted to the above concentrations in PBS supplemented with 5% NDS and incubated on slides in the dark for 2 hours at room temperature. Sections were then washed twice for five minutes in PBS and DAPI was added (1:1000 for 2 minutes). Following DAPI staining, sections were washed for 5 minutes in ddH20 and then mounted with a coverslip.

All sections were imaged with an Aperio ImageScope and analyzed using an algorithm developed with Aperio IndicaLabs- CytoNuclear FLv1.2 software. The algorithm is designed to take into account factors such as nuclear staining, cytoplasm radius, nucelar size, nuclear roundness, and dye fluorescence wavelength (Cy2, Cy3, or Cy5), to identify, differentiate, and count β, δ, and α cells. The algorithm was also used to count the number of β-, δ-, and α- cells on the slides labeled with Brd-U, which was further analyzed using ImageJ software and Microsoft Excel.

Statistics

The data is presented as recordings that are averaged or representative of results obtained from at least three independent cultures. All values presented are the mean ± SEM. Statistical differences between means were assessed using Student's *t*-test or one-way ANOVA, as appropriate. The significance of all experimental findings presented as fold changes was assessed by performing statistical tests on log-transformed data. $P<0.05$ was considered as significant.

Supplementary Material

Refer to Web version on PubMed Central for supplementary material.

Acknowledgments

We are grateful for the helpful discussions and input from the laboratory of Dr. Al Powers. We would like to thank Dr. Matthew Merrins, University of Wisconsin – Madison, for sharing reagents used for ER Ca^{2+} imaging experiments and for critical review of the manuscript; Dr. Tullio Pozzan, University of Padua, for providing pCMV-D4ER plasmid; and Salma Omer for her contributions to Ca^{2+} imaging experiments performed during this study. Human islets were procured through the Integrated Islet Distribution Program organized by NIDDK. We acknowledge the assistance of the Vanderbilt Translational Pathology Shared Resource in the preparation and processing of paraffin-embedded pancreata (2P30 CA068485-14; 5U24DK059637-13). Imaging and analysis of stained pancreas sections was performed with the assistance of the Vanderbilt Islet Procurement and Analysis Core (DK020593). **Funding:** This project was funded by National Institutes of Health grants K01DK081666, R01DK097392, Vanderbilt Diabetes Research and Training Center Pilot and Feasibility Grant P60DK20593, and American Diabetes Association grant 1-17-IBS-024 (D.A.J.); Vanderbilt Molecular Endocrinology Training Program (METP) grant 5T32DK07563 and National Institutes of Health grant 1F31DK109625 (N.C.V.); Vanderbilt METP grant 5T32DK007563-28 (S.C.M.); and Vanderbilt Integrated Training in Engineering and Diabetes grant T32DK101003 (M.T.D.). P.G. is Research Director of the Fonds de la Recherche Scientifique-FNRS, Brussels, Belgium. Confocal microscopy was performed using the Vanderbilt Cell Imaging Shared Resource (DK020593).

References

1. Gilon P, Chae HY, Rutter GA, Ravier MA. Calcium signaling in pancreatic beta-cells in health and in Type 2 diabetes. Cell Calcium. 2014; 56:340–361. [PubMed: 25239387]
2. Santulli G, Pagano G, Sardu C, Xie W, Reiken S, D'Ascia SL, Cannone M, Marziliano N, Trimarco B, Guise TA, Lacampagne A, Marks AR. Calcium release channel RyR2 regulates insulin release and glucose homeostasis. The Journal of Clinical Investigation. 2015; 125:1968–1978. [PubMed: 25844899]
3. Ramadan JW, Steiner SR, O'Neill CM, Nunemaker CS. The central role of calcium in the effects of cytokines on beta-cell function: implications for type 1 and type 2 diabetes. Cell Calcium. 2011; 50:481–490. [PubMed: 21944825]
4. Johnson JS, Kono T, Tong X, Yamamoto WR, Zarain-Herzberg A, Merrins MJ, Satin LS, Gilon P, Evans-Molina C. Pancreatic and duodenal homeobox protein 1 (Pdx-1) maintains endoplasmic reticulum calcium levels through transcriptional regulation of sarco-endoplasmic reticulum calcium

ATPase 2b (SERCA2b) in the islet beta cell. The Journal of Biological Chemistry. 2014; 289:32798–32810. [PubMed: 25271154]

5. Roe MW, Philipson LH, Frangakis CJ, Kuznetsov A, Mertz RJ, Lancaster ME, Spencer B, Worley JF 3rd, Dukes ID. Defective glucose-dependent endoplasmic reticulum Ca^{2+} sequestration in diabetic mouse islets of Langerhans. The Journal of Biological Chemistry. 1994; 269:18279–18282. [PubMed: 8034570]
6. O'Neill CM, Lu C, Corbin KL, Sharma PR, Dula SB, Carter JD, Ramadan JW, Xin W, Lee JK, Nunemaker CS. Circulating levels of IL-1B+IL-6 cause ER stress and dysfunction in islets from prediabetic male mice. Endocrinology. 2013; 154:3077–3088. [PubMed: 23836031]
7. Cardozo AK, Ortis F, Storling J, Feng YM, Rasschaert J, Tonnesen M, Van Eylen F, Mandrup-Poulsen T, Herchuelz A, Eizirik DL. Cytokines downregulate the sarcoendoplasmic reticulum pump Ca^{2+} ATPase 2b and deplete endoplasmic reticulum Ca^{2+}, leading to induction of endoplasmic reticulum stress in pancreatic beta-cells. Diabetes. 2005; 54:452–461. [PubMed: 15677503]
8. Fonseca SG, Ishigaki S, Oslowski CM, Lu S, Lipson KL, Ghosh R, Hayashi E, Ishihara H, Oka Y, Permutt MA, Urano F. Wolfram syndrome 1 gene negatively regulates ER stress signaling in rodent and human cells. The Journal of Clinical Investigation. 2010; 120:744–755. [PubMed: 20160352]
9. Tengholm A, Gylfe E. Oscillatory control of insulin secretion. Molecular and Cellular Endocrinology. 2009; 297:58–72. [PubMed: 18706473]
10. Arruda AP, Pers BM, Parlakgul G, Guney E, Inouye K, Hotamisligil GS. Chronic enrichment of hepatic endoplasmic reticulum-mitochondria contact leads to mitochondrial dysfunction in obesity. Nat Med. 2014; 20:1427–1435. [PubMed: 25419710]
11. Ozcan U, Yilmaz E, Ozcan L, Furuhashi M, Vaillancourt E, Smith RO, Gorgun CZ, Hotamisligil GS. Chemical chaperones reduce ER stress and restore glucose homeostasis in a mouse model of type 2 diabetes. Science. 2006; 313:1137–1140. [PubMed: 16931765]
12. Xiao C, Giacca A, Lewis GF. Sodium phenylbutyrate, a drug with known capacity to reduce endoplasmic reticulum stress, partially alleviates lipid-induced insulin resistance and beta-cell dysfunction in humans. Diabetes. 2011; 60:918–924. [PubMed: 21270237]
13. McKinley D, Meissner G. Evidence for a K^+, Na^+ permeable channel in sarcoplasmic reticulum. The Journal of Membrane Biology. 1978; 44:159–186. [PubMed: 731686]
14. Kuum M, Veksler V, Kaasik A. Potassium fluxes across the endoplasmic reticulum and their role in endoplasmic reticulum calcium homeostasis. Cell Calcium. 2015; 58:79–85. [PubMed: 25467968]
15. Guo T, Nani A, Shonts S, Perryman M, Chen H, Shannon T, Gillespie D, Fill M. Sarcoplasmic reticulum K(+) (TRIC) channel does not carry essential countercurrent during Ca(2+) release. Biophysical Journal. 2013; 105:1151–1160. [PubMed: 24010658]
16. Yazawa M, Ferrante C, Feng J, Mio K, Ogura T, Zhang M, Lin PH, Pan Z, Komazaki S, Kato K, Nishi M, Zhao X, Weisleder N, Sato C, Ma J, Takeshima H. TRIC channels are essential for Ca^{2+} handling in intracellular stores. Nature. 2007; 448:78–82. [PubMed: 17611541]
17. Yamazaki D, Tabara Y, Kita S, Hanada H, Komazaki S, Naitou D, Mishima A, Nishi M, Yamamura H, Yamamoto S, Kakizawa S, Miyachi H, Yamamoto S, Miyata T, Kawano Y, Kamide K, Ogihara T, Hata A, Umemura S, et al. TRIC-A channels in vascular smooth muscle contribute to blood pressure maintenance. Cell Metabolism. 2011; 14:231–241. [PubMed: 21803293]
18. Yamazaki D, Komazaki S, Nakanishi H, Mishima A, Nishi M, Yazawa M, Yamazaki T, Taguchi R, Takeshima H. Essential role of the TRIC-B channel in Ca^{2+} handling of alveolar epithelial cells and in perinatal lung maturation. Development. 2009; 136:2355–2361. [PubMed: 19515693]
19. Zhao C, Ichimura A, Qian N, Iida T, Yamazaki D, Noma N, Asagiri M, Yamamoto K, Komazaki S, Sato C, Aoyama F, Sawaguchi A, Kakizawa S, Nishi M, Takeshima H. Mice lacking the intracellular cation channel TRIC-B have compromised collagen production and impaired bone mineralization. Sci Signal. 2016; 9:ra49. [PubMed: 27188440]
20. Kuum M, Veksler V, Liiv J, Ventura-Clapier R, Kaasik A. Endoplasmic reticulum potassium-hydrogen exchanger and small conductance calcium-activated potassium channel activities are essential for ER calcium uptake in neurons and cardiomyocytes. Journal of Cell Science. 2012; 125:625–633. [PubMed: 22331352]
21. Renigunta V, Yuan H, Zuzarte M, Rinne S, Koch A, Wischmeyer E, Schlichthorl G, Gao Y, Karschin A, Jacob R, Schwappach B, Daut J, Preisig-Muller R. The retention factor p11 confers an

endoplasmic reticulum-localization signal to the potassium channel TASK-1. Traffic. 2006; 7:168–181. [PubMed: 16420525]

22. Kilisch M, Lytovchenko O, Schwappach B, Renigunta V, Daut J. The role of protein-protein interactions in the intracellular traffic of the potassium channels TASK-1 and TASK-3. Pflugers Archiv : European Journal of Physiology. 2015; 467:1105–1120. [PubMed: 25559843]
23. Ashmole I, Goodwin PA, Stanfield PR. TASK-5, a novel member of the tandem pore K^+ channel family. Pflugers Archiv : European Journal of Physiology. 2001; 442:828–833. [PubMed: 11680614]
24. Chatelain FC, Bichet D, Feliciangeli S, Larroque MM, Braud VM, Douguet D, Lesage F. Silencing of the tandem pore domain halothane-inhibited K^+ channel 2 (THIK2) relies on combined intracellular retention and low intrinsic activity at the plasma membrane. The Journal of Biological Chemistry. 2013; 288:35081–35092. [PubMed: 24163367]
25. Lesage F, Lazdunski M. Molecular and functional properties of two-pore-domain potassium channels. Am J Physiol Renal Physiol. 2000; 279:F793–801. [PubMed: 11053038]
26. Huttlin EL, Ting L, Bruckner RJ, Gebreab F, Gygi MP, Szpyt J, Tam S, Zarraga G, Colby G, Baltier K, Dong R, Guarani V, Vaites LP, Ordureau A, Rad R, Erickson BK, Wuhr M, Chick J, Zhai B, et al. The BioPlex Network: A Systematic Exploration of the Human Interactome. Cell. 2015; 162:425–440. [PubMed: 26186194]
27. Dickerson MT, Vierra NC, Milian SC, Dadi PK, Jacobson DA. Osteopontin activates the diabetes-associated potassium channel TALK-1 in pancreatic beta-cells. PloS one. 2017; 12:e0175069. [PubMed: 28403169]
28. Vierra NC, Dadi PK, Jeong I, Dickerson M, Powell DR, Jacobson DA. Type 2 Diabetes-Associated K^+ Channel TALK-1 Modulates beta-Cell Electrical Excitability, Second-Phase Insulin Secretion, and Glucose Homeostasis. Diabetes. 2015; 64:3818–3828. [PubMed: 26239056]
29. Stitzel ML, Sethupathy P, Pearson DS, Chines PS, Song L, Erdos MR, Welch R, Parker SC, Boyle AP, Scott LJ, Program NCS, Margulies EH, Boehnke M, Furey TS, Crawford GE, Collins FS. Global epigenomic analysis of primary human pancreatic islets provides insights into type 2 diabetes susceptibility loci. Cell Metabolism. 2010; 12:443–455. [PubMed: 21035756]
30. Ku GM, Kim H, Vaughn IW, Hangauer MJ, Myung Oh C, German MS, McManus MT. Research resource: RNA-Seq reveals unique features of the pancreatic beta-cell transcriptome. Molecular Endocrinology. 2012; 26:1783–1792. [PubMed: 22915829]
31. Benner C, van der Meulen T, Caceres E, Tigyi K, Donaldson CJ, Huising MO. The transcriptional landscape of mouse beta cells compared to human beta cells reveals notable species differences in long non-coding RNA and protein-coding gene expression. BMC Genomics. 2014; 15:620. [PubMed: 25051960]
32. Bramswig NC, Everett LJ, Schug J, Dorrell C, Liu C, Luo Y, Streeter PR, Naji A, Grompe M, Kaestner KH. Epigenomic plasticity enables human pancreatic alpha to beta cell reprogramming. The Journal of Clinical Investigation. 2013; 123:1275–1284. [PubMed: 23434589]
33. Li J, Klughammer J, Farlik M, Penz T, Spittler A, Barbieux C, Berishvili E, Bock C, Kubicek S. Single-cell transcriptomes reveal characteristic features of human pancreatic islet cell types. EMBO Reports. 2016; 17:178–187. [PubMed: 26691212]
34. Cho YS, Chen CH, Hu C, Long J, Ong RT, Sim X, Takeuchi F, Wu Y, Go MJ, Yamauchi T, Chang YC, Kwak SH, Ma RC, Yamamoto K, Adair LS, Aung T, Cai Q, Chang LC, Chen YT, et al. Meta-analysis of genome-wide association studies identifies eight new loci for type 2 diabetes in east Asians. Nature Genetics. 2012; 44:67–72.
35. Mahajan A, Go MJ, Zhang W, Below JE, Gaulton KJ, Ferreira T, Horikoshi M, Johnson AD, Ng MC, Prokopenko I, Saleheen D, Wang X, Zeggini E, et al. D. I. G. Replication, C. Meta-analysis, C. Asian Genetic Epidemiology Network Type 2 Diabetes, C. South Asian Type 2 Diabetes, C. Mexican American Type 2 Diabetes, C. Type 2 Diabetes Genetic Exploration by Nex-generation sequencing in muylti-Ethnic Samples. Genome-wide trans-ancestry meta-analysis provides insight into the genetic architecture of type 2 diabetes susceptibility. Nature Genetics. 2014; 46:234–244. [PubMed: 24509480]
36. Muller YL, Piaggi P, Chen P, Wiessner G, Okani C, Kobes S, Knowler WC, Bogardus C, Hanson RL, Baier LJ. Assessing Variation across Eight Established East Asian Loci for Type 2 Diabetes in

American Indians: Suggestive Evidence for New Sex-specific Diabetes Signals in GLIS3 and ZFAND3. Diabetes Metab Res Rev. 2016

37. Suzuki J, Kanemaru K, Ishii K, Ohkura M, Okubo Y, Iino M. Imaging intraorganellar Ca2+ at subcellular resolution using CEPIA. Nature Communications. 2014; 5:4153.
38. Ravier MA, Daro D, Roma LP, Jonas JC, Cheng-Xue R, Schuit FC, Gilon P. Mechanisms of control of the free Ca^{2+} concentration in the endoplasmic reticulum of mouse pancreatic beta-cells: interplay with cell metabolism and $[Ca^{2+}]_C$ and role of SERCA2b and SERCA3. Diabetes. 2011; 60:2533–2545. [PubMed: 21885870]
39. Solovyova N, Veselovsky N, Toescu EC, Verkhratsky A. Ca(2+) dynamics in the lumen of the endoplasmic reticulum in sensory neurons: direct visualization of Ca(2+)-induced Ca(2+) release triggered by physiological Ca(2+) entry. The EMBO Journal. 2002; 21:622–630. [PubMed: 11847110]
40. Sharma RB, O'Donnell AC, Stamateris RE, Ha B, McCloskey KM, Reynolds PR, Arvan P, Alonso LC. Insulin demand regulates beta cell number via the unfolded protein response. The Journal of Clinical Investigation. 2015; 125:3831–3846. [PubMed: 26389675]
41. Stamateris RE, Sharma RB, Hollern DA, Alonso LC. Adaptive beta-cell proliferation increases early in high-fat feeding in mice, concurrent with metabolic changes, with induction of islet cyclin D2 expression. American Journal of Physiology. Endocrinology and Metabolism. 2013; 305:E149–159. [PubMed: 23673159]
42. Han J, Kang D, Kim D. Functional properties of four splice variants of a human pancreatic tandem-pore K^+ channel, TALK-1. American Journal of Physiology. Cell Physiology. 2003; 285:C529–538. [PubMed: 12724142]
43. Dadi PK, Vierra NC, Days EL, Dickerson M, Vinson PN, Weaver CD, Jacobson DA. Selective small molecule activators of TREK-2 channels stimulate DRG c-fiber nociceptor K2P currents and limit calcium influx. ACS Chem Neurosci. 2016
44. Bandara S, Malmersjo S, Meyer T. Regulators of calcium homeostasis identified by inference of kinetic model parameters from live single cells perturbed by siRNA. Sci Signal. 2013; 6:ra56. [PubMed: 23838183]
45. Flaherty DP, Simpson DS, Miller M, Maki BE, Zou B, Shi J, Wu M, McManus OB, Aube J, Li M, Golden JE. Potent and selective inhibitors of the TASK-1 potassium channel through chemical optimization of a bis-amide scaffold. Bioorg Med Chem Lett. 2014; 24:3968–3973. [PubMed: 25017033]
46. Dadi PK, Luo B, Vierra NC, Jacobson DA. TASK-1 potassium channels limit pancreatic alpha-cell calcium influx and glucagon secretion. Molecular Endocrinology. 2015 me20141321.
47. Ma L, Roman-Campos D, Austin ED, Eyries M, Sampson KS, Soubrier F, Germain M, Tregouet DA, Borczuk A, Rosenzweig EB, Girerd B, Montani D, Humbert M, Loyd JE, Kass RS, Chung WK. A novel channelopathy in pulmonary arterial hypertension. N Engl J Med. 2013; 369:351–361. [PubMed: 23883380]
48. Abramcheck CW, Best PM. Physiological role and selectivity of the in situ potassium channel of the sarcoplasmic reticulum in skinned frog skeletal muscle fibers. The Journal of General Physiology. 1989; 93:1–21. [PubMed: 2915210]
49. Gillespie D, Fill M. Intracellular calcium release channels mediate their own countercurrent: the ryanodine receptor case study. Biophysical Journal. 2008; 95:3706–3714. [PubMed: 18621826]
50. Mak DO, Vais H, Cheung KH, Foskett JK. Nuclear patch-clamp electrophysiology of Ca^{2+} channels. Cold Spring Harb Protoc. 2013; 2013:885–891. [PubMed: 24003194]
51. Gilon P, Arredouani A, Gailly P, Gromada J, Henquin JC. Uptake and release of Ca^{2+} by the endoplasmic reticulum contribute to the oscillations of the cytosolic Ca^{2+} concentration triggered by Ca^{2+} influx in the electrically excitable pancreatic B-cell. The Journal of Biological Chemistry. 1999; 274:20197–20205. [PubMed: 10400636]
52. Arredouani A, Henquin JC, Gilon P. Contribution of the endoplasmic reticulum to the glucose-induced [Ca(2+)](c) response in mouse pancreatic islets. American Journal of Physiology. Endocrinology and Metabolism. 2002; 282:E982–991. [PubMed: 11934662]

53. Goforth PB, Bertram R, Khan FA, Zhang M, Sherman A, Satin LS. Calcium-activated K^+ channels of mouse beta-cells are controlled by both store and cytoplasmic Ca^{2+}: experimental and theoretical studies. The Journal of General Physiology. 2002; 120:307–322. [PubMed: 12198088]
54. Gopel SO, Kanno T, Barg S, Eliasson L, Galvanovskis J, Renstrom E, Rorsman P. Activation of Ca(2+)-dependent K(+) channels contributes to rhythmic firing of action potentials in mouse pancreatic beta cells. The Journal of General Physiology. 1999; 114:759–770. [PubMed: 10578013]
55. Rolland JF, Henquin JC, Gilon P. Feedback control of the ATP-sensitive K(+) current by cytosolic Ca(2+) contributes to oscillations of the membrane potential in pancreatic beta-cells. Diabetes. 2002; 51:376–384. [PubMed: 11812744]
56. Dufer M, Gier B, Wolpers D, Krippeit-Drews P, Ruth P, Drews G. Enhanced glucose tolerance by SK4 channel inhibition in pancreatic beta-cells. Diabetes. 2009; 58:1835–1843. [PubMed: 19401418]
57. Zhang M, Houamed K, Kupershmidt S, Roden D, Satin LS. Pharmacological properties and functional role of Kslow current in mouse pancreatic beta-cells: SK channels contribute to Kslow tail current and modulate insulin secretion. The Journal of General Physiology. 2005; 126:353–363. [PubMed: 16186562]
58. Emmanouilidou E, Teschemacher AG, Pouli AE, Nicholls LI, Seward EP, Rutter GA. Imaging Ca^{2+} concentration changes at the secretory vesicle surface with a recombinant targeted cameleon. Curr Biol. 1999; 9:915–918. [PubMed: 10469598]
59. Girard C, Duprat F, Terrenoire C, Tinel N, Fosset M, Romey G, Lazdunski M, Lesage F. Genomic and functional characteristics of novel human pancreatic 2P domain K(+) channels. Biochemical and Biophysical Research Communications. 2001; 282:249–256. [PubMed: 11263999]
60. Kono T, Ahn G, Moss DR, Gann L, Zarain-Herzberg A, Nishiki Y, Fueger PT, Ogihara T, Evans-Molina C. PPAR-gamma activation restores pancreatic islet SERCA2 levels and prevents beta-cell dysfunction under conditions of hyperglycemic and cytokine stress. Molecular Endocrinology. 2012; 26:257–271. [PubMed: 22240811]
61. Tong X, Kono T, Evans-Molina C. Nitric oxide stress and activation of AMP-activated protein kinase impair beta-cell sarcoendoplasmic reticulum calcium ATPase 2b activity and protein stability. Cell Death Dis. 2015; 6:e1790. [PubMed: 26086963]
62. Tong X, Kono T, Anderson-Baucum EK, Yamamoto W, Gilon P, Lebeche D, Day RN, Shull GE, Evans-Molina C. SERCA2 Deficiency Impairs Pancreatic beta-Cell Function in Response to Diet-Induced Obesity. Diabetes. 2016; 65:3039–3052. [PubMed: 27489309]
63. Chang-Chen KJ, Mullur R, Bernal-Mizrachi E. Beta-cell failure as a complication of diabetes. Rev Endocr Metab Disord. 2008; 9:329–343. [PubMed: 18777097]
64. Caspersen C, Pedersen PS, Treiman M. The sarco/endoplasmic reticulum calcium-ATPase 2b is an endoplasmic reticulum stress-inducible protein. The Journal of Biological Chemistry. 2000; 275:22363–22372. [PubMed: 10748035]
65. Thuerauf DJ, Hoover H, Meller J, Hernandez J, Su L, Andrews C, Dillmann WH, McDonough PM, Glembotski CC. Sarco/endoplasmic reticulum calcium ATPase-2 expression is regulated by ATF6 during the endoplasmic reticulum stress response: intracellular signaling of calcium stress in a cardiac myocyte model system. The Journal of Biological Chemistry. 2001; 276:48309–48317. [PubMed: 11595740]
66. Li M, Baumeister P, Roy B, Phan T, Foti D, Luo S, Lee AS. ATF6 as a transcription activator of the endoplasmic reticulum stress element: thapsigargin stress-induced changes and synergistic interactions with NF-Y and YY1. Molecular and Cellular Biology. 2000; 20:5096–5106. [PubMed: 10866666]
67. Wang Y, Shen J, Arenzana N, Tirasophon W, Kaufman RJ, Prywes R. Activation of ATF6 and an ATF6 DNA binding site by the endoplasmic reticulum stress response. The Journal of Biological Chemistry. 2000; 275:27013–27020. [PubMed: 10856300]
68. Marmugi A, Parnis J, Chen X, Carmichael L, Hardy J, Mannan N, Marchetti P, Piemonti L, Bosco D, Johnson P, Shapiro JA, Cruciani-Guglielmacci C, Magnan C, Ibberson M, Thorens B, Valdivia HH, Rutter GA, Leclerc I. Sorcin Links Pancreatic beta-Cell Lipotoxicity to ER Ca^{2+} Stores. Diabetes. 2016; 65:1009–1021. [PubMed: 26822088]

69. Luciani DS, Gwiazda KS, Yang TL, Kalynyak TB, Bychkivska Y, Frey MH, Jeffrey KD, Sampaio AV, Underhill TM, Johnson JD. Roles of IP3R and RyR Ca^{2+} channels in endoplasmic reticulum stress and beta-cell death. Diabetes. 2009; 58:422–432. [PubMed: 19033399]
70. Varadi A, Rutter GA. Dynamic imaging of endoplasmic reticulum Ca^{2+} concentration in insulin-secreting MIN6 Cells using recombinant targeted cameleons: roles of sarco(endo)plasmic reticulum Ca^{2+}-ATPase (SERCA)-2 and ryanodine receptors. Diabetes. 2002; 51(Suppl 1):S190–201. [PubMed: 11815480]
71. Cassel R, Ducreux S, Alam MR, Dingreville F, Berle C, Burda-Jacob K, Chauvin MA, Chikh K, Paita L, Al-Mawla R, Crola Da Silva C, Rieusset J, Thivolet C, Van Coppenolle F, Madec AM. Protection of Human Pancreatic Islets from Lipotoxicity by Modulation of the Translocon. PloS One. 2016; 11:e0148686. [PubMed: 26862742]
72. Ng KE, Schwarzer S, Duchen MR, Tinker A. The intracellular localization and function of the ATP-sensitive K^+ channel subunit Kir6.1. The Journal of Membrane Biology. 2010; 234:137–147. [PubMed: 20306027]
73. Henquin JC, Ishiyama N, Nenquin M, Ravier MA, Jonas JC. Signals and pools underlying biphasic insulin secretion. Diabetes. 2002; 51(Suppl 1):S60–67. [PubMed: 11815460]
74. Arredouani A, Guiot Y, Jonas JC, Liu LH, Nenquin M, Pertusa JA, Rahier J, Rolland JF, Shull GE, Stevens M, Wuytack F, Henquin JC, Gilon P. SERCA3 ablation does not impair insulin secretion but suggests distinct roles of different sarcoendoplasmic reticulum Ca(2+) pumps for Ca(2+) homeostasis in pancreatic beta-cells. Diabetes. 2002; 51:3245–3253. [PubMed: 12401716]
75. Tamarina NA, Kuznetsov A, Rhodes CJ, Bindokas VP, Philipson LH. Inositol (1,4,5)-trisphosphate dynamics and intracellular calcium oscillations in pancreatic beta-cells. Diabetes. 2005; 54:3073–3081. [PubMed: 16249428]
76. Dula SB, Jecmenica M, Wu R, Jahanshahi P, Verrilli GM, Carter JD, Brayman KL, Nunemaker CS. Evidence that low-grade systemic inflammation can induce islet dysfunction as measured by impaired calcium handling. Cell Calcium. 2010; 48:133–142. [PubMed: 20800281]
77. Miura Y, Henquin JC, Gilon P. Emptying of intracellular Ca^{2+} stores stimulates Ca^{2+} entry in mouse pancreatic beta-cells by both direct and indirect mechanisms. The Journal of Physiology. 1997; 503(Pt 2):387–398. [PubMed: 9306280]
78. Tengholm A, Hellman B, Gylfe E. The endoplasmic reticulum is a glucose-modulated high-affinity sink for Ca^{2+} in mouse pancreatic beta-cells. The Journal of Physiology. 2001; 530:533–540. [PubMed: 11158282]
79. Cnop M, Abdulkarim B, Bottu G, Cunha DA, Igoillo-Esteve M, Masini M, Turatsinze JV, Griebel T, Villate O, Santin I, Bugliani M, Ladriere L, Marselli L, McCarthy MI, Marchetti P, Sammeth M, Eizirik DL. RNA sequencing identifies dysregulation of the human pancreatic islet transcriptome by the saturated fatty acid palmitate. Diabetes. 2014; 63:1978–1993. [PubMed: 24379348]
80. Sutendra G, Dromparis P, Wright P, Bonnet S, Haromy A, Hao Z, McMurtry MS, Michalak M, Vance JE, Sessa WC, Michelakis ED. The role of Nogo and the mitochondria-endoplasmic reticulum unit in pulmonary hypertension. Sci Transl Med. 2011; 3:88ra55.
81. Dromparis P, Paulin R, Stenson TH, Haromy A, Sutendra G, Michelakis ED. Attenuating endoplasmic reticulum stress as a novel therapeutic strategy in pulmonary hypertension. Circulation. 2013; 127:115–125. [PubMed: 23149668]
82. Antigny F, Hautefort A, Meloche J, Belacel-Ouari M, Manoury B, Rucker-Martin C, Pechoux C, Potus F, Nadeau V, Tremblay E, Ruffenach G, Bourgeois A, Dorfmuller P, Breuils-Bonnet S, Fadel E, Ranchoux B, Jourdon P, Girerd B, Montani D, et al. Potassium Channel Subfamily K Member 3 (KCNK3) Contributes to the Development of Pulmonary Arterial Hypertension. Circulation. 2016; 133:1371–1385. [PubMed: 26912814]
83. Yao J, McHedlishvili D, McIntire WE, Guagliardo NA, Erisir A, Coburn CA, Santarelli VP, Bayliss DA, Barrett PQ. Functional TASK-3-Like Channels in Mitochondria of Aldosterone-Producing Zona Glomerulosa Cells. Hypertension. 2017; 70:347–356. [PubMed: 28630209]
84. Xian Tao L, Dyachenko V, Zuzarte M, Putzke C, Preisig-Muller R, Isenberg G, Daut J. The stretch-activated potassium channel TREK-1 in rat cardiac ventricular muscle. Cardiovasc Res. 2006; 69:86–97. [PubMed: 16248991]

85. Ma D, Jan LY. ER transport signals and trafficking of potassium channels and receptors. Current Opinion in Neurobiology. 2002; 12:287–292. [PubMed: 12049935]

86. Hille B, Dickson EJ, Kruse M, Vivas O, Suh BC. Phosphoinositides regulate ion channels. Biochim Biophys Acta. 2015; 1851:844–856. [PubMed: 25241941]

87. Wilke BU, Lindner M, Greifenberg L, Albus A, Kronimus Y, Bunemann M, Leitner MG, Oliver D. Diacylglycerol mediates regulation of TASK potassium channels by Gq-coupled receptors. Nature Communications. 2014; 5:5540.

88. Dadi PK, Vierra NC, Jacobson DA. Pancreatic beta-Cell-specific Ablation of TASK-1 Channels Augments Glucose-stimulated Calcium Entry and Insulin Secretion, Improving Glucose Tolerance. Endocrinology. 2014; 155:3757–3768. [PubMed: 24932805]

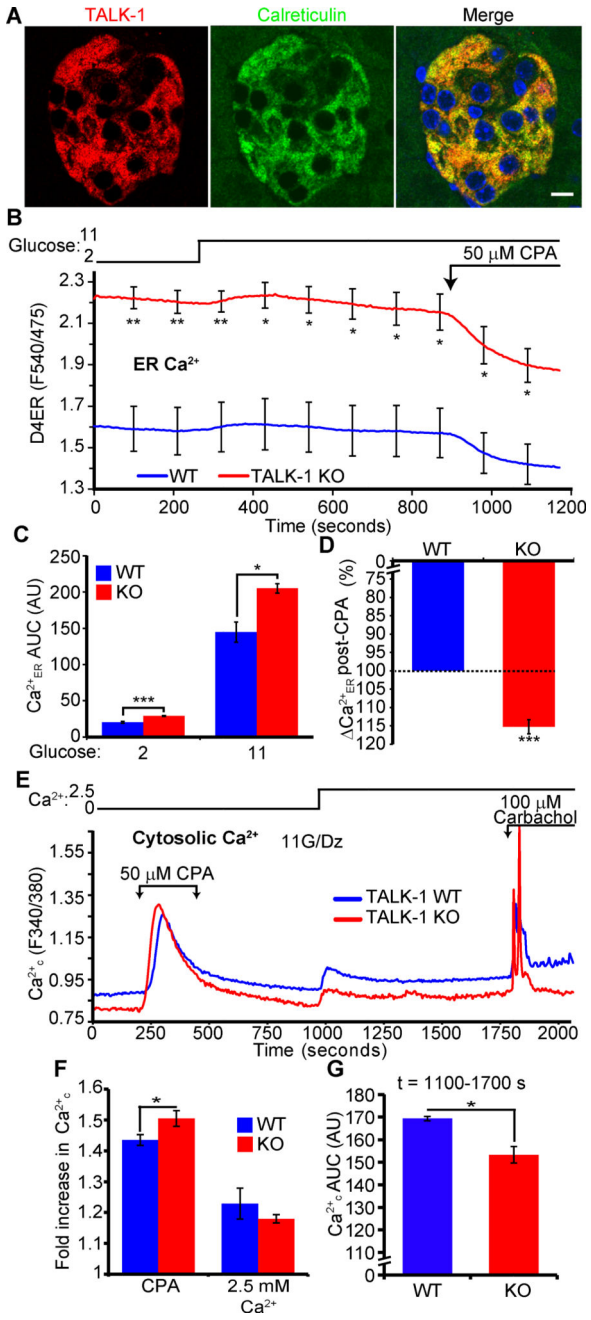

Figure 1. TALK-1 channels modulate β-cell Ca^{2+}_{ER} homeostasis

(**A**) Representative images of a mouse pancreas section stained for TALK-1 and calreticulin. Scale bar is 10 μm. Images are representative of results obtained from 3 mice. (**B**) β-cell Ca^{2+}_{ER} measurements made with the genetically encoded Ca^{2+}_{ER} indicator D4ER. Cells were perfused with solutions containing indicated glucose concentrations and 50 μM CPA (N = 3 mice per genotype). (**C**) Area under the curve (AUC) analysis of Ca^{2+}_{ER} under low (2 mM) and high (11 mM) glucose conditions from (B). (**D**) CPA-induced reduction in Ca^{2+}_{ER}, presented as percent of maximum Ca^{2+}_{ER} of wild-type (WT) β-cells from (B). (**E**) WT and TALK-1 KO β-cells were perfused with the indicated solutions; 11 mM glucose (G)

and 125 μM diazoxide (Dz) were present throughout the experiment. (**F**) Fold increase in Ca^{2+} in response to the indicated treatments. (**G**) Ca^{2+} AUC for the period following addition of 2.5 mM Ca^{2+} to the extracellular buffer (t=1000–1750 s) (N = 5 mice per genotype for E to G). Statistical significance was determined by Student's t-test; *P<0.05, **P<0.01, ***P<0.005.

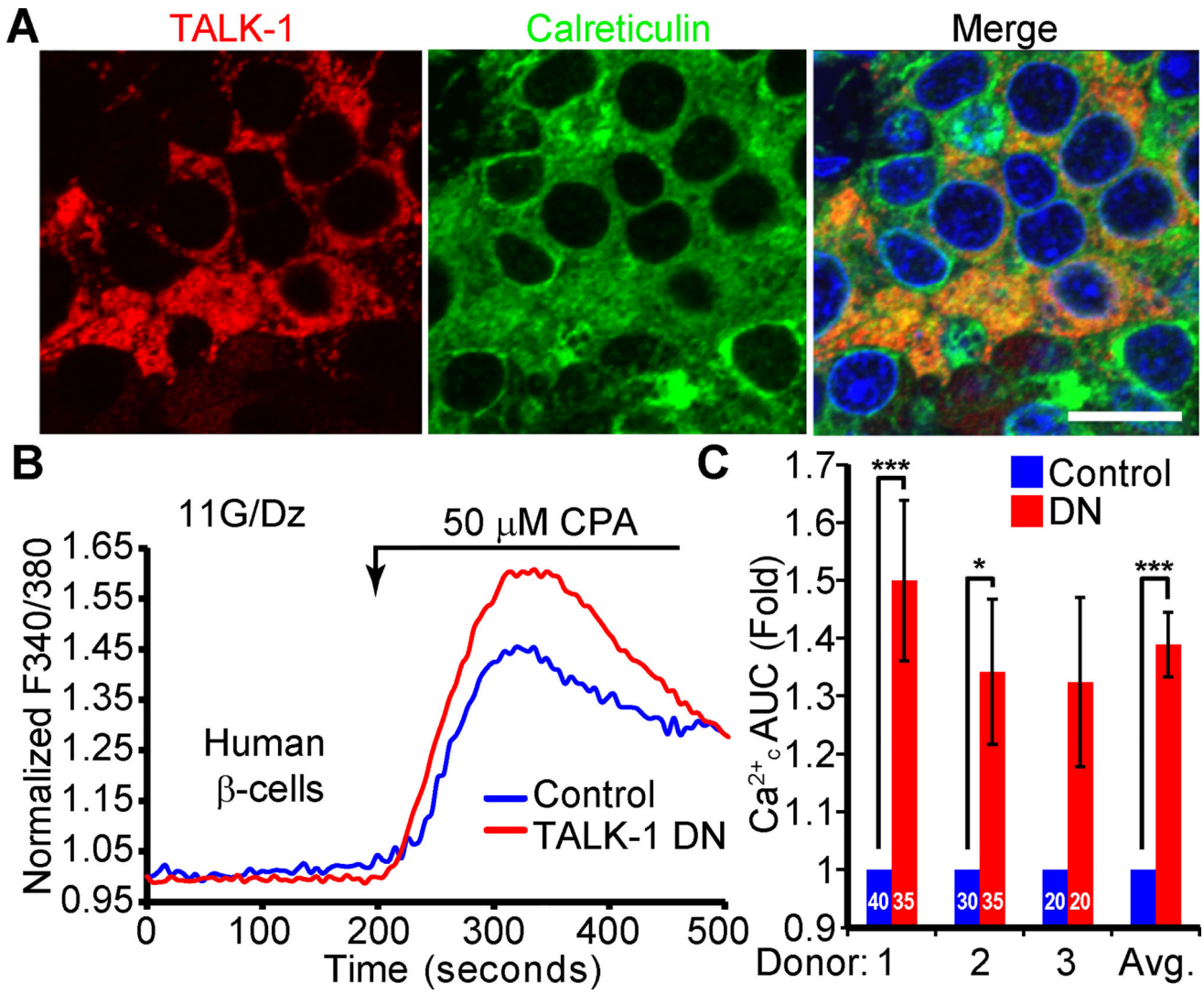

Figure 2. TALK-1 channels modulate human β-cell Ca^{2+}_{ER} homeostasis

(**A**) Representative image of a human pancreas section stained for TALK-1 and calreticulin. Scale bar is 10 μm. (**B**) Representative recordings of intracellular Ca^{2+} in human β-cells transfected with either TALK-1 dominant negative mutant (DN) or mCherry control. 11 mM glucose (G), 0 mM Ca^{2+}, 125 μM diazoxide (Dz), and 1 mM EGTA were present throughout. (**C**) Quantification of the fold change in the Ca^{2+} AUC in response to treatment with CPA in human β-cells. The number of β-cells per donor are indicated on the graph. Statistical significance was determined by Student's *t*-test and one-way ANOVA followed by Bonferroni's multiple comparison test; **P*<0.05, ***P*<0.01, ****P*<0.005.

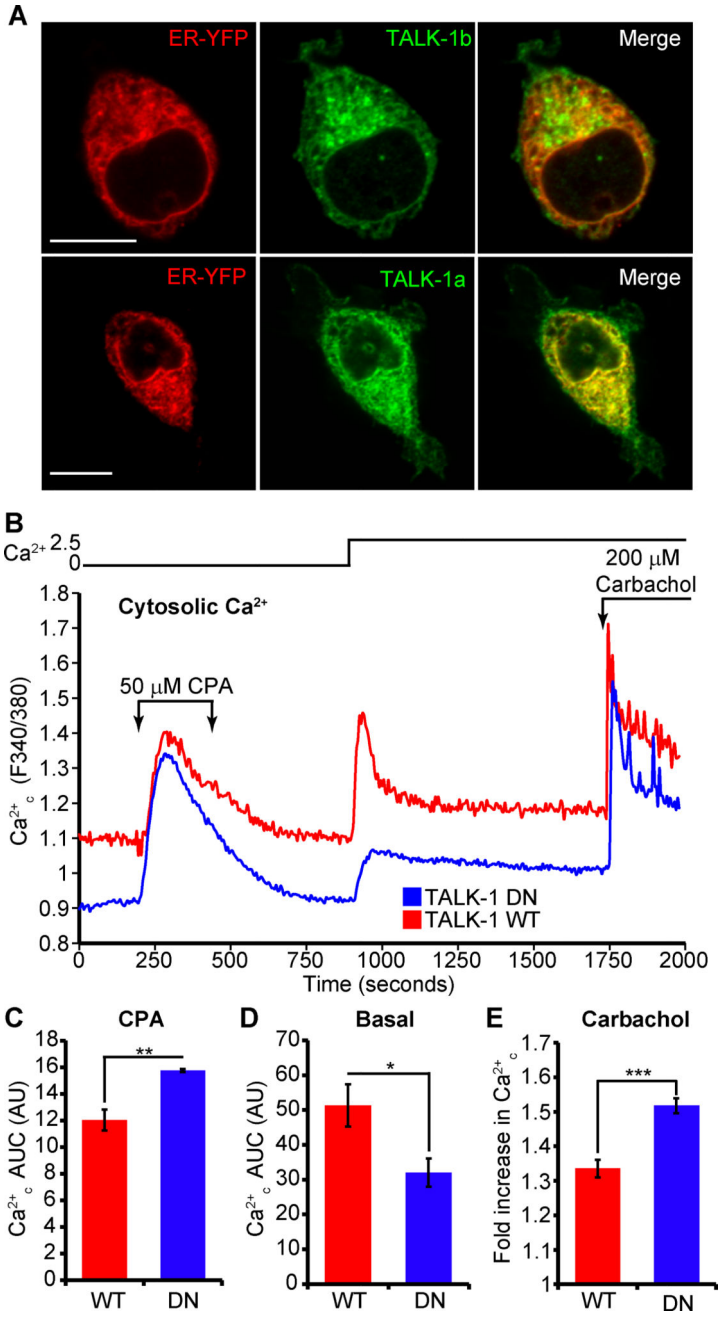

Figure 3. The K^+ channel function of TALK-1 contributes to its regulation of Ca^{2+}_{ER} homeostasis

(**A**) TALK-1b and -1a co-localize with the ER marker ER-YFP. Images are representative of 3 independent experiments. Scale bar is 10 μm. (**B**) Representative recordings of HEK293 cells expressing either WT TALK-1 or TALK-1 DN and perfused with the indicated solutions; 10 mM glucose was present throughout the experiment. (**C**) Normalized Ca^{2+} AUC for the period during treatment with CPA (t=250–600 s). (**D**) Ca^{2+} AUC for the period following addition of 2.5 mM Ca^{2+} to the extracellular buffer (t=1000–1750 s). (**E**) Fold increase in Ca^{2+} in response to treatment with the muscarinic receptor agonist carbachol (*N*

= 3 independent experiments for B to D). Statistical significance was determined by Student's *t*-test; **P*<0.05, ***P*<0.01, ****P*<0.005.

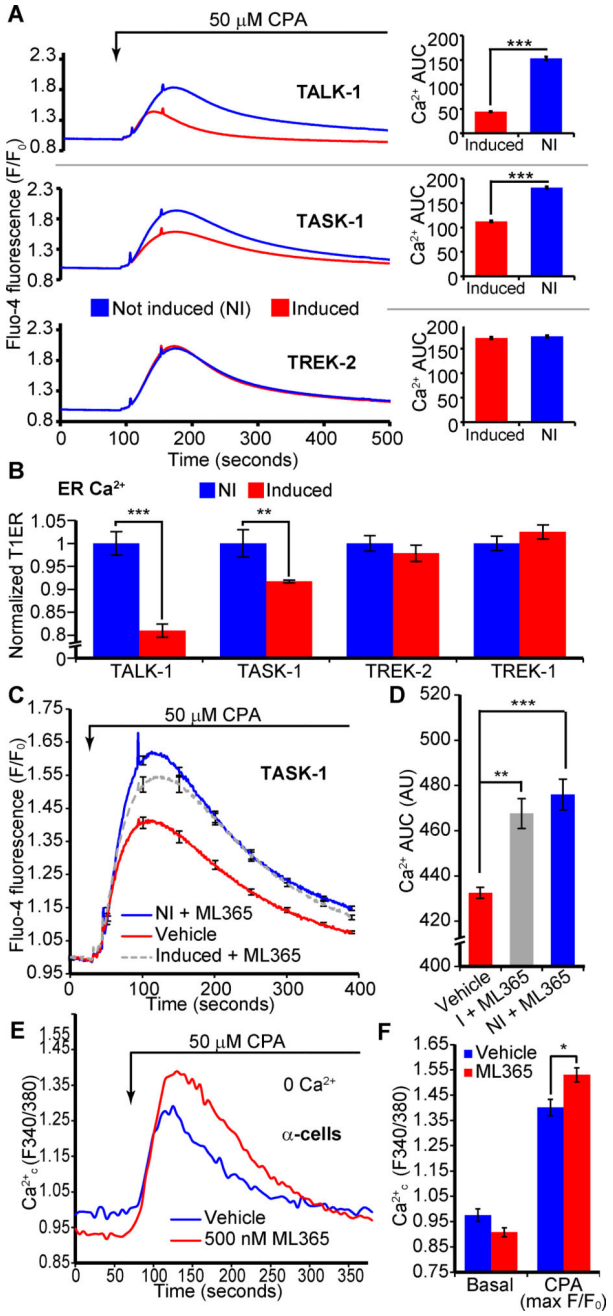

Figure 4. Pharmacological manipulation of K2P channel activity can alter steady-state Ca^{2+}_{ER} concentrations

(**A**) Representative recordings of CPA-induced Ca^{2+}_{ER} release in cell lines with tetracycline-inducible expression of the indicated K2P channels. Ca^{2+} AUC in response to CPA is shown to the right (representative of $N = 3$ independent experiments; NI: not induced). (**B**) Direct quantification of Ca^{2+}_{ER} concentration in HEK293 cells with inducible expression of TALK-1, TASK-1, TREK-2, TREK-1 and the Ca^{2+}_{ER} indicator T1ER ($N = 3$ independent experiments). (**C** and **D**) Treatment of TASK-1-expressing cells with ML365 restores Ca^{2+}_{ER} to pre-channel expression concentrations (C); AUC quantification (D) ($N = 3$

independent experiments). (**E**) Mouse α-cells were treated with ML365 in the presence of 11 mM glucose and 125 μM diazoxide (representative of $N = 3$ independent experiments). The response to CPA is quantified in (**F**) ($N = 3$ independent experiments). Statistical significance was determined by Student's *t*-test; *$P<0.05$, **$P<0.01$, ***$P<0.005$.

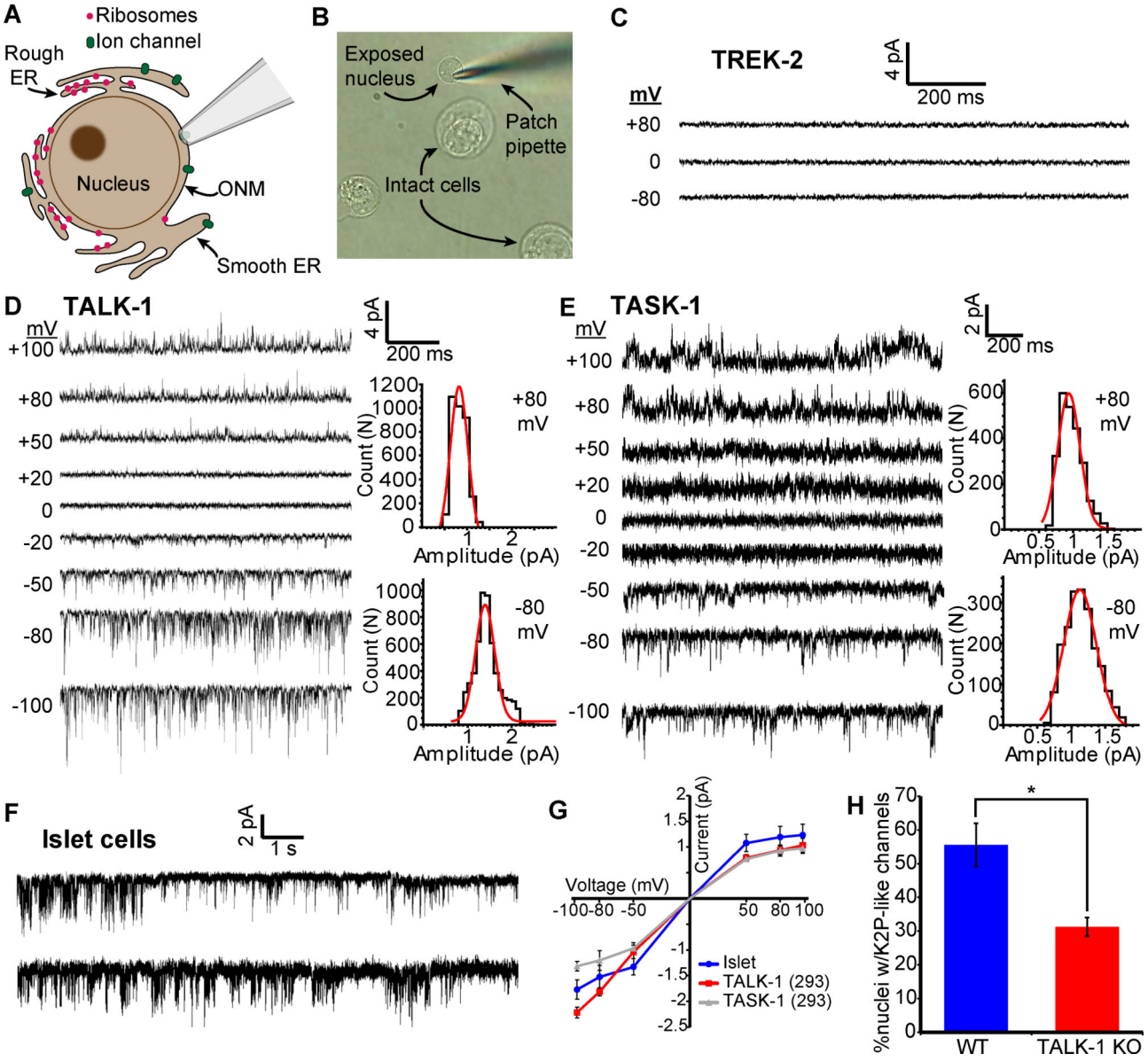

Figure 5. Functional TALK-1 and TASK-1 channels are present in the ER membrane

(**A**) Nuclear patch clamp of the outer nuclear membrane (ONM) permits detection of ER ion channels. (**B**) Representative image of isolated mouse islet nuclei with patch pipette positioned on nucleus. (**C**) Recordings obtained from the nucleus of a TREK-2-expressing HEK293 cell (representative of 5 nuclei). (**D**) Current trace obtained from the nucleus of a TALK-1 expressing HEK293 cell. Representative current amplitude histograms at right (representative of 8 nuclei). (**E**) As in **D**, but recorded from the nucleus of a TASK-1 expressing cell (representative of 7 nuclei). (**F**) Representative current traces obtained from WT mouse nuclei; patches held at −50 mV (representative of 42 nuclei) (**G**) Single-channel current-voltage relationships from nucleus recordings obtained from TALK-1- ($N = 8$) and TASK-1- ($N = 7$) expressing HEK293 cells and WT islet-cells ($N = 42$). (**H**) Percent of nuclei with K2P-channel-like channel activity detected in WT and TALK-1 KO β-cells ($N =$

42 nuclei; 4 mice per genotype). Statistical significance was determined by Student's *t*-test; $*P<0.05$.

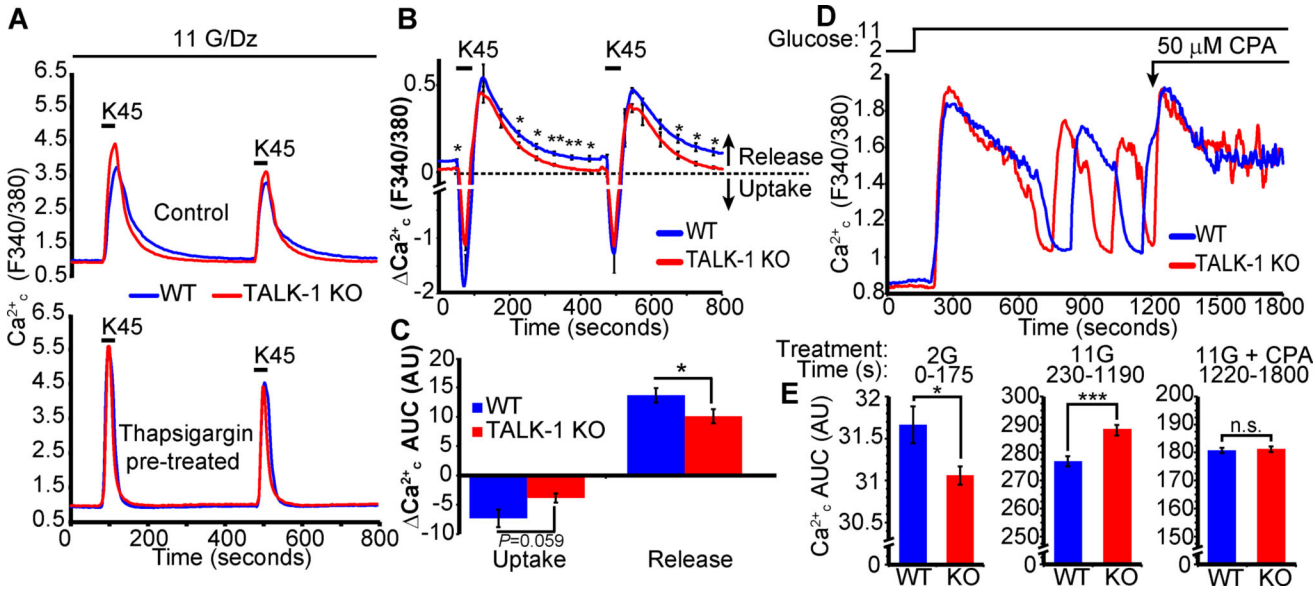

Figure 6. TALK-1 regulates Ca^{2+}_{ER} handling during plasma membrane Ca^{2+} influx in β-cells

(**A**) Intracellular Ca^{2+} oscillations in response to pulses of 45 mM K^+ (K45) for 40 seconds in the presence or absence of thapsigargin (1.25 μM). Recordings were performed in the presence of 11 mM glucose (G), 2.5 mM Ca^{2+}, and 125 μM diazoxide (Dz). (**B**) Subtraction of the thapsigargin-treated trace from the control trace in A reveals the kinetics of Ca^{2+}_{ER} uptake and release. (**C**) Quantification of average Ca^{2+}_{ER} uptake and release in WT and TALK-1 KO β-cells (*N* = 3 mice per genotype). (**D**) Effect of CPA on glucose-stimulated Ca^{2+} influx in WT and KO islets. (**E**) Area under the curve (AUC) analysis of glucose-stimulated Ca^{2+} influx for periods corresponding to low glucose (2G), high glucose (11G), and CPA (11G + CPA) (*N* = 49 WT and 53 TALK-1 KO islets). Statistical significance was determined by Student's *t*-test; **P*<0.05, ***P*<0.01, ****P*<0.005.

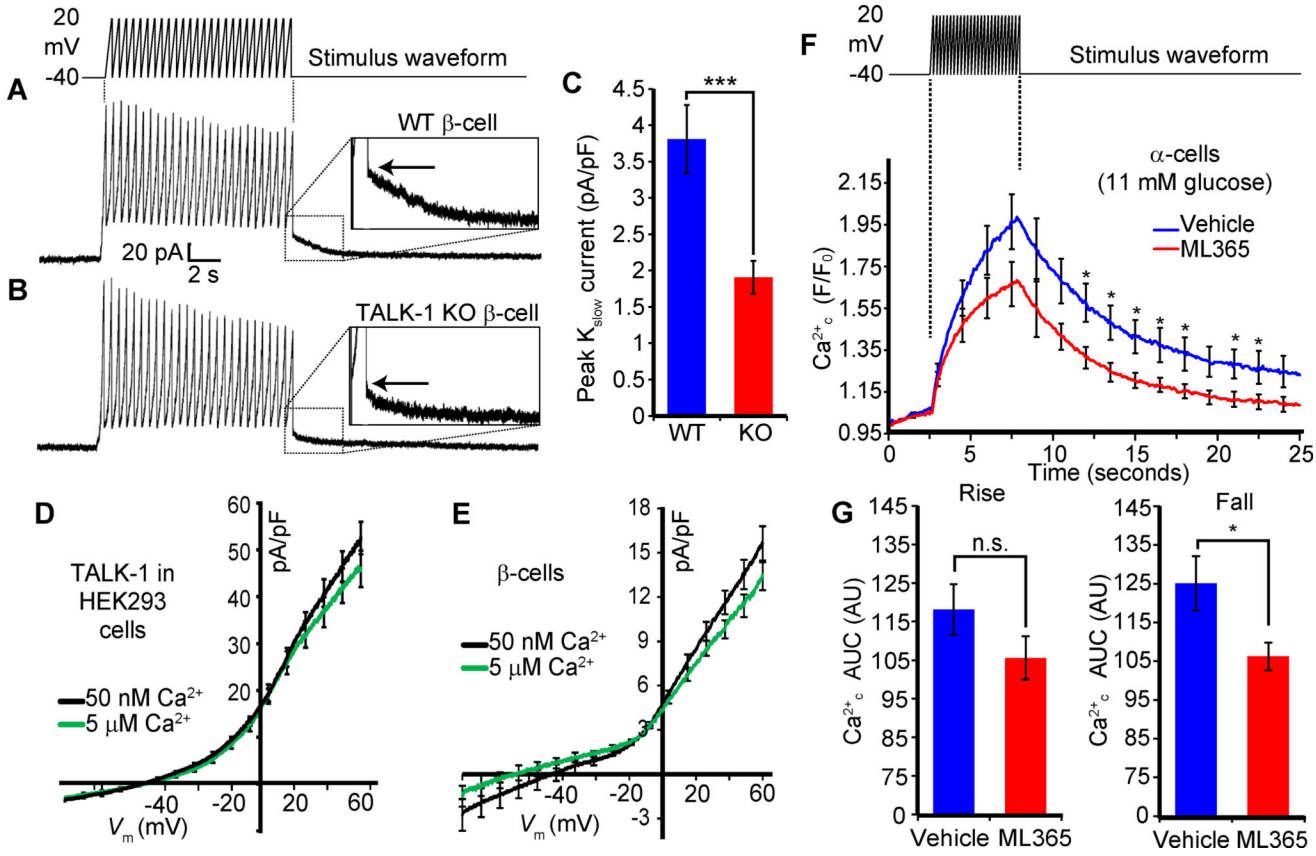

Figure 7. Reduced K_{slow} currents are associated with altered Ca^{2+}_{ER} dynamics

(**A** and **B**) Representative K_{slow} currents recorded from WT (**A**) and TALK-1 KO (**B**) β-cells. The peak of the K_{slow} tail current is indicated by the arrow. (**C**) Quantification of K_{slow} currents recorded from WT and TALK-1 KO β-cells (N = 26 cells; 4 mice per genotype). (**D** and **E**) Average whole-cell currents recorded in HEK293 cells expressing TALK-1 with intracellular buffer containing low Ca^{2+} (50 nM, black line) or high Ca^{2+} (5 μM, green line) in HEK293 (**D**, N = 11 cells per condition) and mouse β-cells (**E**, N = 15 (50 nM Ca^{2+}) and 13 cells (5 μM)). (**F**) Depolarization-induced Ca^{2+} influx in mouse α-cells treated with vehicle or ML365. (**G**) AUC analysis of rising (rise) and decaying (fall) phase of Ca^{2+} influx in α-cells suggests reduced Ca^{2+}-induced Ca^{2+}_{ER} release in ML365-treated α-cells (N = 11 cells per condition). Statistical significance was determined by Student's t-test; *P<0.05, ***P<0.005.

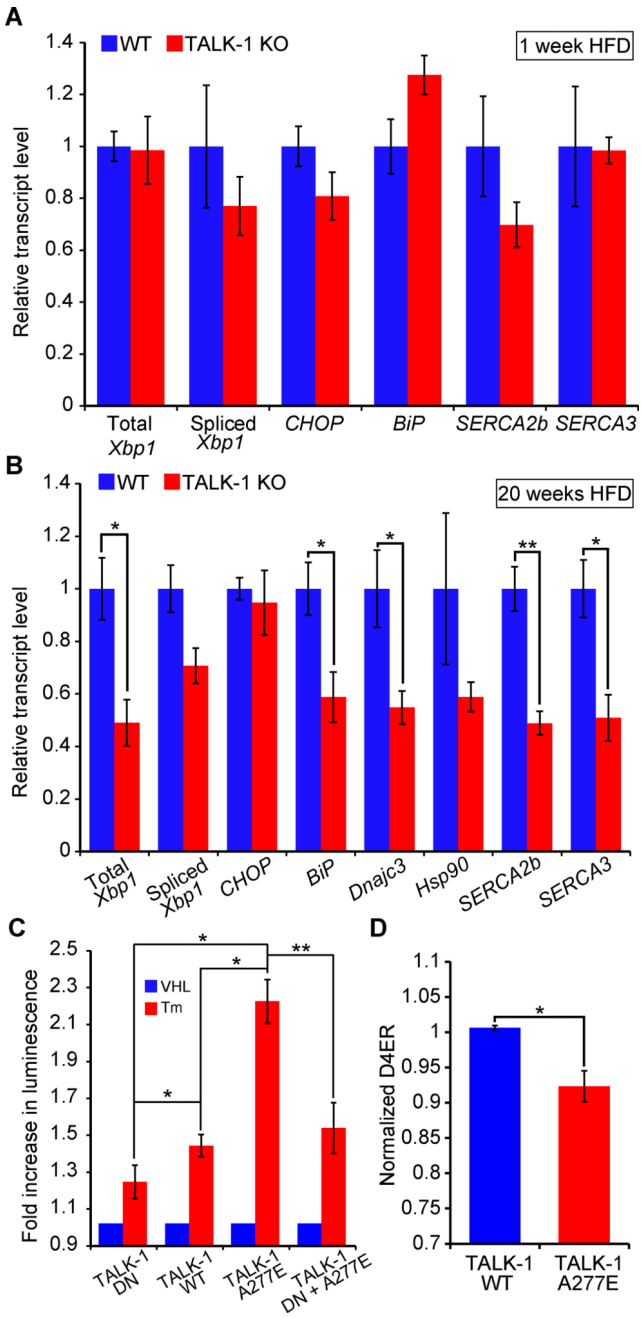

Figure 8. TALK-1 channel activity exacerbates ER stress

(**A**) Reverse-transcribed RNA from islets isolated from wild-type (WT) and TALK-1 KO mice fed a HFD for 1 week was subjected to quantitative real-time PCR (qRT-PCR) to measure total *Xbp1*, spliced *Xbp1, CHOP, BiP, Atp2a2* (SERCA2b), and *Atp2a3* (SERCA3) expression ($N = 4–5$ mice per genotype). (**B**) Reverse-transcribed RNA from islets isolated from wild-type (WT) and TALK-1 KO mice fed a HFD for 20 weeks was subjected to qRT-PCR to measure total *Xbp1*, spliced *Xbp1, CHOP, BiP, Dnajc3, Hsp90, Atp2a2* (SERCA2b), and *Atp2a3* (SERCA3) expression ($N = 3–4$ mice per genotype). (**C**) INS-1 cells co-transfected with TALK-1 DN mutant, wild-type TALK-1 (WT), or TALK-1 A277E and an

ATF6 promoter luciferase reporter (p5×ATF6-GL3) were treated with vehicle (VHL) (DMSO, 0.0125% v/v) or tunicamycin (Tm) (0.25 μg/mL) for 16–20 hours prior to cell lysis and luciferase assay ($N = 4$ independent experiments). (**D**) INS-1 cells were co-transfected with TALK-1 WT or TALK-1 A277E and pCMV-D4ER to measure basal Ca^{2+}_{ER} concentrations in 11 mM glucose ($N = 4$ independent experiments). Statistical significance was determined by Student's *t*-test; *$P<0.05$, **$P<0.01$.